An inventory of rock glaciers in the central British Columbia Coast Mountains, Canada, from high resolution Google Earth imagery

Ansley A. Charbonneau & Dan J. Smith

2018

Arctic, Antarctic, and Alpine Research

An Interdisciplinary Journal

ISSN: 1523-0430 (Print) 1938-4246 (Online) Journal homepage: https://www.tandfonline.com/loi/uaar20

An inventory of rock glaciers in the central British Columbia Coast Mountains, Canada, from high resolution Google Earth imagery

Ansley A. Charbonneau & Dan J. Smith

To cite this article: Ansley A. Charbonneau & Dan J. Smith (2018) An inventory of rock glaciers in the central British Columbia Coast Mountains, Canada, from high resolution Google Earth imagery, Arctic, Antarctic, and Alpine Research, 50:1, e1489026, DOI: 10.1080/15230430.2018.1489026

To link to this article: https://doi.org/10.1080/15230430.2018.1489026

ARCTIC, ANTARCTIC, AND ALPINE RESEARCH
2018, VOL. 50, NO. 1, e1489026 (24 pages)
https://doi.org/10.1080/15230430.2018.1489026

Taylor & Francis
Taylor & Francis Group

An inventory of rock glaciers in the central British Columbia Coast Mountains, Canada, from high resolution Google Earth imagery

Ansley A. Charbonneau and Dan J. Smith

Department of Geography, University of Victoria, British Columbia, Canada

ABSTRACT

Little is known about the presence, distribution, age, or activity of rock glaciers in the British Columbia Coast Mountains of western Canada. Reflecting debris accumulation and mass wasting under a periglacial climate, these rock glaciers describe a geomorphic response to permafrost regimes that may or may not presently exist. An inventory of rock glacier landforms in the eastern front ranges of the Coast Mountains, using high-resolution Google Earth imagery, documented 165 rock glaciers between lat. 50°10′ and 52°08′ N. The majority of these rock glaciers occur at sites positioned between 1,900 and 2,300 m above sea level, where rain shadow effects and continental air masses result in persistent dry, cold conditions. Morphology and field observation suggest that these features contain intact ice. The rock glaciers occupy predominately northwest- to northeast-facing slopes, with talus-derived rock glaciers largely restricted to north-facing slopes. Glacier-derived features outnumber talus-derived features by a ratio of 5:1. Several of the inventoried rock glaciers were located up valley from presumed Younger Dryas terminal moraines, indicating that they formed after 9390 BP. Dendrogeomorphological investigations at one rock glacier record contemporary activity that resulted in 1.3 cm/yr of frontal advance since AD 1674. This inventory is the first to document the presence of rock glaciers in the Coast Mountains and supports preliminary understandings of permafrost distribution in the southwestern Canadian Cordillera.

ARTICLE HISTORY
Received 13 March 2017
Revised 27 May 2018
Accepted 5 June 2018

KEYWORDS
Rock glacier; British Columbia Coast Mountains; periglacial; permafrost; tree rings

Introduction

The British Columbia Coast Mountains flank the Pacific coast of western Canada, rising from sea level to more than 4,000 m in the Mt. Waddington area (Figure 1). Along their windward maritime slopes, deep winter snow packs persist into the summer months, allowing for the development of high-elevation ice fields and large valley glaciers. Eastward glaciers decrease in size and number, because strong rain shadow effects result in a subcontinental environment in the front ranges abutting the Chilcotin Plateau. While ice fields are absent in the front ranges and glaciers are largely restricted to shaded northeast-facing high-elevation cirques (Falconer, Henoch, and Østrem 1965; Østrem 1966; Østrem and Arnold 1970), satellite imagery shows that rock glaciers of varying size and morphology are abundant.

Little is known about the presence, distribution, age, or activity of rock glaciers in the Coast Mountains (French and Slaymaker 1993). Reflecting debris accumulation and mass wasting under a periglacial climate (Haeberli et al. 2006; Humlum 2000), their occurrence describes a geomorphic response to permafrost thermal regimes that may or may not presently exist (Humlum 1998). While a provisional map suggests that much of the region is currently favorable for the development and persistence of permafrost (Hasler, Geertsma, and Hoelzle 2014), it remains to be determined whether these landforms are the fossilized remains of rock glaciers active during Late Pleistocene or Holocene permafrost conditions or whether they illustrate a geomorphic response to present-day permafrost environments.

The intent of this research was to document the distribution and general characteristics of rock glaciers in the southeastern front ranges of the Coast Mountains. We hypothesized that the spatial and altitudinal distribution of rock glaciers in this region would allow for interpretation of their paleohistory in the context of Holocene climatic variability, and would allow for further understanding of the present-day occurrence of permafrost within this setting. To achieve these objectives, the

CONTACT Dan J. Smith smith@uvic.ca

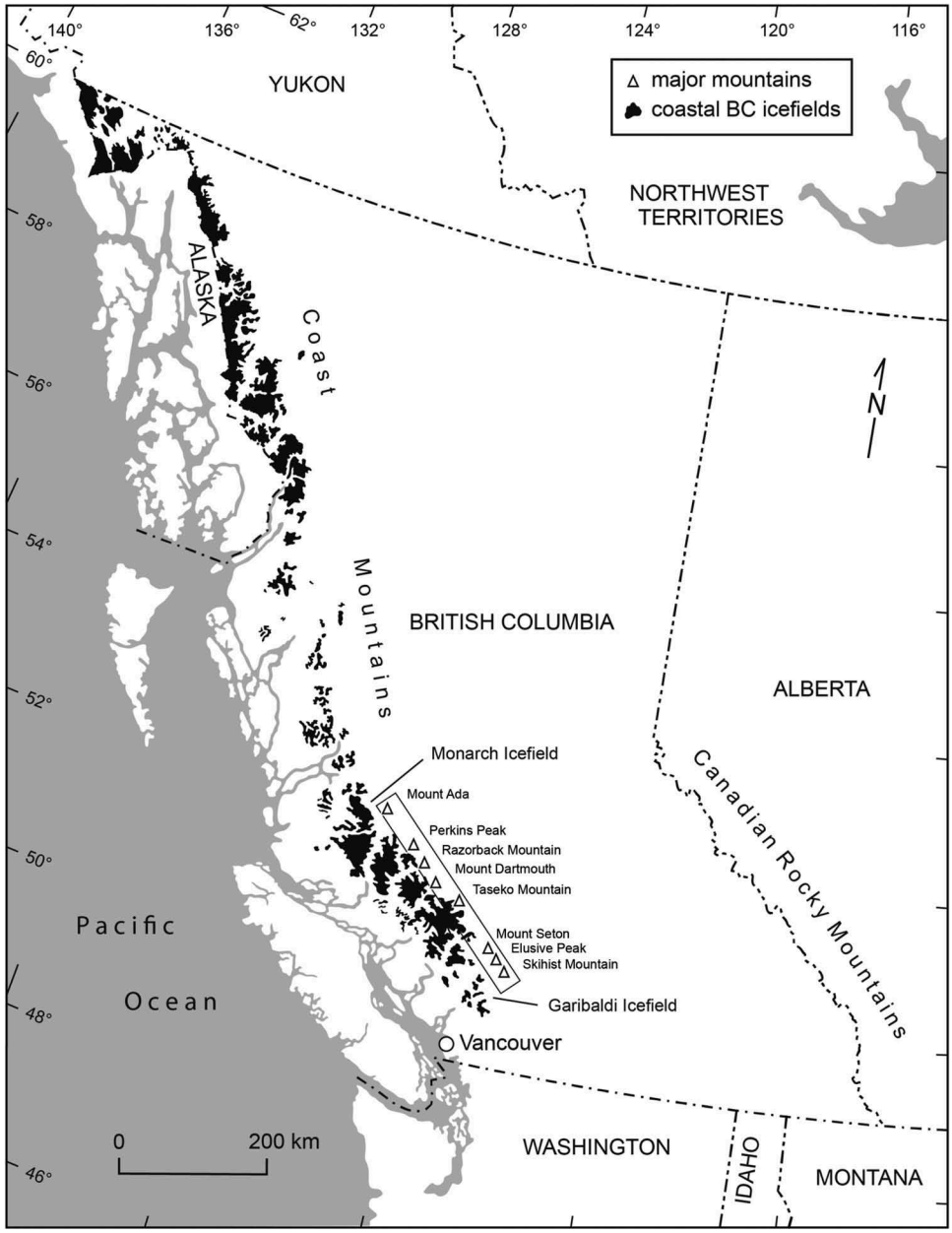

Figure 1. Map of British Columbia, Canada, showing the location of the front ranges study area. Mountain peaks are provided for geographic reference.

characteristics of a large sample of rock glaciers from the region are compared to regional climatic gradients and topographic conditions. Dendrochronology was used at one rock glacier site to gain an understanding of contemporary rock glacier geomorphology.

Research background

The term *rock glacier* is associated with a range of landform types found in arctic and alpine environments (Janke et al. 2013). By definition, rock glaciers consist of perennially frozen masses of ice and debris that creep downslope under the weight of gravity (Barsch 1996; Haeberli 1985; Haeberli et al. 2006). Transverse ridges and longitudinal furrows are the surface expression of this internal ice deformation (Barsch 1996; Frehner, Ling, and Gärtner-Roer 2014).

The surface of most rock glaciers consists of a seasonally thawed active layer characterized by angular boulders and large interstitial spaces. This debris mantle acts as a filter between external climatic conditions and the permanently frozen interior below the permafrost table (Haeberli et al. 2006; Humlum 1996; Wahrhaftig and Cox 1959). Cold, dense air settles in

the interstitial spaces between the rocks and cools the permafrost despite short-term surface fluctuations in snow cover and above 0°C air temperatures (Humlum 1997). Rock glaciers, therefore, provide evidence of the lower extent of permafrost because of their ability to maintain a frozen state despite the general trend of warmer mean annual air temperatures at lower elevations (Boeckli et al. 2012; Lilleøren and Etzelmuller 2011; Lilleøren et al. 2013a; Scotti et al. 2013).

In high mountain regions, rock glaciers commonly form at sites characterized by cool air temperatures and moderate amounts of precipitation (Haeberli 1985; Humlum 1998). While rock glaciers are occasionally found in maritime climate regions (Humlum 1982; Lilleøren et al. 2013a; Martin and Whalley 1987), their distribution is largely restricted to continental climate zones. Rain shadow conditions are ideal for rock glacier formation, as the thin mountain snowpack that characterizes many of these regions reduces insulation, allowing cold winter air temperatures to sustain negative ground temperatures (Haeberli et al. 2006; Humlum 1997). In mountainous settings rock glaciers are most commonly located were shading shields them from insolation and the local topography directs cold winds down into the debris layer (Humlum 1997, 1998).

Previous descriptions of rock glaciers in the western Canadian Cordillera focus on those found in the southern Canadian Rocky Mountains in Alberta (Bachrach et al. 2004; Carter et al. 1999; Gardner 1978; Koning and Smith 1999; Luckman and Crockett 1978; Osborn 1975), as well as in the St. Elias and Selwyn Mountains in Yukon (Johnson 1978, 1980; Sloan and Dyke 1998). The majority of rock glaciers in the southern Canadian Rocky Mountains are located in high-elevation, north-facing cirques where the local lithology exerts a strong control on their form and presence. In that area, rock glaciers are common in the shales and quartzites of the Main Ranges, but are sparse in the shales and carbonates of the Front Ranges (Luckman and Crockett 1978). Most of these rock glaciers are believed to have developed following the retreat of the Cordilleran Ice Sheet at the end of the Pleistocene, although absolute origin ages have not been assigned (Johnson 1978; Luckman and Crockett 1978).

Study area

The study area for this research includes the southeastern Coast Mountain Front Ranges from east of the Garibaldi Icefield (lat. 50°10′ N) to terrain northwest of the Monarch Icefield (lat. 52°08′ N; Figure 1). The region is south of the continuous permafrost limit in western Canada but is assumed to contain isolated patches of permafrost (up to 10%) at the highest altitudes (Brown and Péwé 1973; Hasler, Geertsma, and Hoelzle 2014; Heginbottom, Dubreuil, and Harker 1995; Rodenhuis et al. 2007). Mean annual air temperatures (1969–1990) range between −5°C and 0°C at the highest elevations on the lee side of the range, with precipitation totals averaging 750 mm/yr or greater (Dawson, Werner, and Murdock 2008).

The region is located within the Coast Mountain Belt, a major tectonic feature located between the Insular and Intermontane superterranes of western British Columbia that were accreted along the continental margin from Middle Jurassic to Early Cretaceous time (Journeay and Friedman 1993). Deformation and contraction resulted in the deposition of preexisting terranes into metamorphosed thrust sheets intruded with plutons (Bustin et al. 2013; Journeay and Friedman 1993; Monger and Journeay 1994). Pockets of volcanic and sedimentary rocks not consumed by the intrusion remain throughout the region, particularly along the eastern border of the Yalakom fault where they are separated from the neighboring Intermontane Belt (Massey et al. 2005).

Following degradation and downwasting of the Cordilleran Ice Sheet and a Late Pleistocene glacial advance in 10.7–10.5 ka (Grubb 2006; Margold et al. 2013), by 10.0 ka glaciers in the study area had retreated several kilometers upvalley to rarely expand beyond their mountain-front terminal positions through the Holocene (Menounos et al. 2009; Mood and Smith 2015). Intervals of cooler/wetter and warmer/drier climates resulted in only minor ice-front oscillations during the Holocene, at least until the last millennia when Little Ice Age (LIA) climate changes (Larocque and Smith 2005a; Steinman et al. 2014) initiated a period of sustained glacier expansion (Larocque and Smith 2005b; Wood, Smith, and Demuth 2011). In the last century rising air temperatures and variable snowpacks (Dawson, Werner, and Murdock 2008) have resulted in negative mass-balance conditions and significant volumetric losses of glacier ice (Bolch, Menounos, and Wheate 2010; Schiefer, Menounos, and Wheate 2007; VanLooy and Forster 2008). Within the study area, many of the cirque glaciers active during the LIA have melted entirely, and a thick cover of rockfall debris mantles the surface of those that remain.

Methods and data

Rock glacier classification

The rock glacier inventory was completed using high-resolution Google Earth satellite imagery (2004/2005). Google Earth was previously used for rock glacier

identification in the Bolivian Andes and the Hindu Kush-Himalayan region (Rangecroft et al. 2014; Schmid et al. 2014), and in the Coast Mountains it represents the best available imagery for detecting rock glaciers across large spatial areas. Google Earth uses SPOT or products from DigitalGlobe (e.g., IKONOS or Quickbird) that have a spatial resolution close to that of aerial photographs (Schmid et al. 2014). The application geo-rectifies the imagery onto a Digital Terrain Model with an accuracy of up to ±90 m (Rusli, Majid, and Din 2014). Only snow-free and cloud-free imagery was used in the survey, and identification was supplemented with field validation where access permitted.

Rock glaciers were categorized based on genesis and ice presence. It is widely accepted that rock glaciers are transitional features, oftentimes marking the interaction between ice of mixed glacial and periglacial origin (Haeberli et al. 2006; Monnier and Kinnard 2015). For this reason, we used a classification scheme that distinguishes between rock glaciers predominately influenced by slope dynamics, such as rock falls and slides (talus-derived; Figure 2a), and those related to glacial dynamics (glacier-derived; Figure 2b and c). Talus-derived rock glaciers originate from talus slopes directly attached to headwalls (Barsch 1996; Haeberli 1985; Haeberli et al. 2006; Humlum 1984); these are often referred to as "true rock glaciers" in the literature (e.g., Clark et al. 1998). Within the glacier-derived category, two forms are present: (1) rock glaciers originating from glacial debris, such as lateral and terminal moraine deposits (Figure 2b)—these features satisfy Barsch's (1996) classification of "debris rock glaciers" and are comparable to those detailed in previous moraine-derived classification schemes (Lilleøren and Etzelmuller 2011; Lilleøren et al. 2013a)—and (2) rock glaciers that are visually connected to glaciers but lack a defined boundary between the glacier ice and the rock glacier below (Figure 2c). The upper sections of these rock glaciers often contain thermokarst thaw pits or are

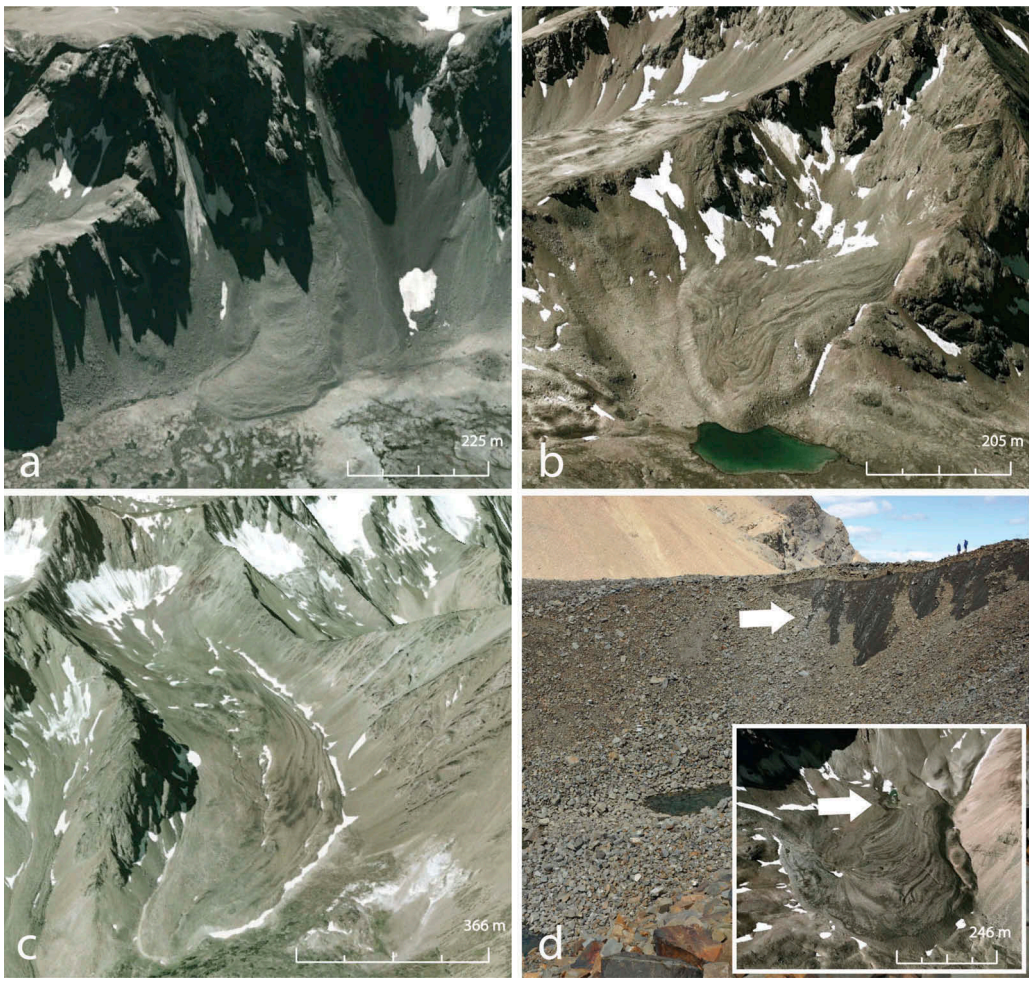

Figure 2. Rock glacier classification: (a) intact talus-derived (ID #98); (b) intact glacier-derived, type A (ID #109); (c) intact glacier-derived, type B (ID #26); and (d) massive ice at Razorback Peak (ID #87). Numbers provided refer to rock glacier ID (see Table 2).

characterized by a depression between the mountainside and the rock glacier deposit. Humlum (1996, 1997) describes similar features in western Greenland, arguing that despite the similarity to glaciers these features display active-layer dynamics and should be termed permafrost landforms. Similar features have been documented in Wyoming (Clark et al. 1998), the Andes of central Chile (Brenning 2005), and in the French Alps (Monnier et al. 2013). The glacier-derived category of rock glaciers includes landforms influenced by glacial activity more broadly, but does not make the claim that these features are of a glacigenic origin (e.g., Berthling 2011; Clark et al. 1998). Massive ice was confirmed at one of the rock glaciers included in our inventory (Figure 2d), supporting the applicability of the glacier-derived classification scheme in this setting.

In an effort to avoid inferring activity from morphology (Berthling 2011), this research considered *intact* rock glaciers as those containing ice and *relict* forms as those with ice no longer present (Haeberli 1985). Only rock glaciers with apparent intact morphology were considered in this study because of the limitations of objective classification without on-the-ground observation. An intact rock glacier was identified as a feature with a steep front at or near the angle of repose with a collection of spilled boulders commonly found in the foreground, indicating surface transport (Barsch 1996; Haeberli 1985). Internal deformation was apparent from ridge/furrow morphology along the surface, and material sorting was visible at the front and sides (Figure 2). Vegetation was not used as an indicator because vegetation has been shown to be present on both intact and relict features (Haeberli 1985; Sorg et al. 2015). While landforms with flatter, thinner fronts and minimal front angles were observed in the study area, these features were not classified as relict. We recognized that shadowing or image resolution could be responsible for the different toe appearance, and direct evidence would be required before these forms could be included in the regional inventory. Furthermore, these features did not appear to be significantly different from intact features in their altitude, aspect, or environmental conditions.

Rock glacier mapping and analysis

The lowermost point of a rock glacier (e.g., toe) was chosen as a discrete boundary between the rock glacier and the surrounding terrain in order to reduce subjectivity in the mapping process. In the case of many glacier-derived rock glaciers, the boundary between glacier, debris-covered ice, and rock glacier was unclear. To prevent an inaccurate estimation of rock glacier extent, the rock glacier toe was used as the best first estimate of rock glacier presence in an area. Additional field reconnaissance would have been necessary to classify many of the transitional features visible in the imagery.

The topographic and climatic characteristics of the rock glaciers identified in the inventory were recorded in a Geographical Information System (GIS) environment (ArcMap 10.0). The coordinate of each rock glacier toe was joined with elevation and aspect layers derived from the Canadian Digital Elevation Model at a resolution of 50 m (Geogratis 2013). In the case of rock glaciers with multiple tongues, the tongue with the lowest elevation was used to obtain a toe coordinate. A digital version of the Geological Map of British Columbia from the British Columbia Ministry of Energy and Mines (1:250,000; Massey et al. 2005) was added to the rock glacier location data to include rock class within the spatial database. Mean annual air temperature (MAAT) and mean annual precipitation (MAP; 1971–2000) data were obtained for each rock glacier toe using ClimateBC (v. 5.04) interpolated weather-station data (Spittlehouse and Wang 2014; Wang et al. 2012). ClimateBC calculates a lapse rate specific to the spatial location, elevation, and variable of interest to produce a scale-free estimate of climatic conditions (Wang et al. 2012).

Environmental conditions were summarized for glacier-derived and talus-derived rock glaciers. Average and standard deviation values were calculated to characterize the populations, followed by pairwise comparisons using the Kruskal-Wallis one-way analysis of variance by ranks for nonparametric data to identify statistically significant differences between categories. All statistical calculations were completed using the software environment R (v. 3.1.2). Circular plots were used to determine the relative spread or concentration of slope aspect across rock glacier categories.

Estimating thermal regimes

In the absence of ground-temperature data from the study area, the spatial distribution of rock glaciers was compared to the location of glaciers and to the position of the upper treeline to estimate the altitudinal extent of periglacial activity (e.g., French and Slaymaker 1993; Harris and Brown 1981). An inverse relationship was assumed to exist between the lower limit of permafrost and the altitude of glaciers (French and Slaymaker 1993). In most cases, where heavy snowfall results in low-lying glaciers near the treeline, the ground is insulated from perennial freezing, and permafrost is restricted to the highest elevations. Conversely, in

continental regions with less precipitation, glaciers form at higher elevations. Permafrost often occurs between the lower limits of glaciation and the contemporary treeline, where the forest cover enhances snow accumulation and insulates the ground (French and Slaymaker 1993).

To facilitate comparison between glaciers, treeline, and rock glaciers at the valley scale, a spatial query selected the closest glacier or treeline position to each rock glacier within a 10 km search distance. The geographic location of glaciers within each search area was derived from the center point of Global Land Ice Measurements from Space (GLIMS) polygons (Racoviteanu et al. 2009) and the upper treeline limit was digitized as a polyline in Google Earth. Mean elevation values for each GLIMS polygon were derived from the 50 m × 50 m Digital Elevation Model (DEM), and treeline elevation was determined using the polyline vertices. The MAAT and MAP for proximal glaciers and the treeline were also gathered using ClimateBC interpolated weather-station data (Spittlehouse and Wang 2014; Wang et al. 2012) to discuss the climatic constrictions associated with discontinuous permafrost distribution. The dependence of MAAT on elevation was tested using a Pearson product-moment correlation coefficient, after which a trend line was used to determine the elevation of the −3°C and 0°C isotherms across the range.

Dendrogeomorphology

Dendrogeomorphological investigations were completed at Hellraving rock glacier (unofficial name) located in the Pantheon Range (51°42′10″ N, 125° 05′22″ W; Figure 1). Hellraving rock glacier is located at the foot of a steep north-facing bedrock wall 5 km south of Hellraving Peak (2,905 m a.s.l.) in the headwaters of Hellraving Creek (51°42′10″ N, 125° 5′23″ W; Figure 3a). Local geologic descriptions are sparse, indicating only that the surficial bedrock is comprised of mid-Cretaceous granitic and gneissic rocks associated with an unnamed pluton (Roddick 1983; van der Heyden, Mustard, and Friedman 1994).

The gently sloping surface (15°) of Hellraving rock glacier is mantled by large angular boulders and covers approximately 0.5 km^2 (1 km long by 0.5 km wide; Figure 3a). The eastern extent of the rock glacier is distinguished by rounded, convoluted ridges beyond which a large depression is evident on the rock glacier surface. Downslope of the depression, a series of transverse ridges suggest that compressional flow has occurred within the lower section of the rock glacier (i.e., Kääb and Weber 2004). Vegetation and lichen were absent on the rock glacier surface.

Sediment sorting is evident on the rock glacier snout and flanks. Larger angular boulders form a 1–2 m thick layer on the surface of the rock glacier, while smaller cobbles and sands extend down the steeply sloping snout to the valley floor at 1,800 m a.s.l. (Figure 3b and 3c). The toe area is surrounded by a mixed forest composed of whitebark pine (*Pinus albicaulis*) and subalpine fir (*Abies lasiocarpa*) trees (Figure 3b). A large pond interspersed with silt deposits and small rock fragments surrounds a portion of the rock glacier snout (Figure 3c).

Boulders that have spilled beyond the rock glacier snout form a characteristic ring of boulders, or "boulder collar" (after Haeberli 1985). While dead and partially buried tree trunks emerge from this debris at several locations (Figure 4), only the northernmost section of the snout appears to be active and advancing into standing trees. Within this area coarse rock debris is spilling down the steep frontal ramp (>30°) to overwhelm and progressively bury trees as the rock glacier advances downslope (Figure 4b). In contrast, most trees located in the eastern extent of the snout appear to have been killed by sporadic boulder topples spilling down moderately sloped talus (<25°) to the valley floor (e.g., Barsch 1996).

Dendrogeomorphological methods were employed to date the historical rate of advance of Hellraving rock glacier into the surrounding forest (e.g., Shroder 1978). Where trees appeared to have been killed by Hellraving rock glacier, their death date was obtained by cross-dating their annual growth rings to living tree-ring chronologies (Giardino, Shroder, and Lawson 1984). An annual rate of movement activity was then assigned by dividing the number of years since the time of death by the horizontal distance to the leading edge of continuous toe debris (Bachrach et al. 2004; Carter et al. 1999).

At Hellraving rock glacier partially buried rooted stumps and trunks were excavated, and cross-sections of the stems were cut with a chainsaw (Figure 5). The horizontal distance from the root position to the debris edge was either directly measured or estimated where excavation was not possible. The tree samples were returned to the University of Victoria Tree-Ring Laboratory (UVTRL) where they were allowed to air dry, and tree species were identified using bark and anatomical characteristics (Hoadley 1990). Following this, the samples were sanded to a fine polish to highlight the annual ring boundaries. The samples were then scanned with a high-resolution scanner to obtain digital images, and the annual ring widths were measured along the longest pathway with a WinDendro (v. 2012c) image-processing measurement system (Guay, Gagnon, and Morin 1992).

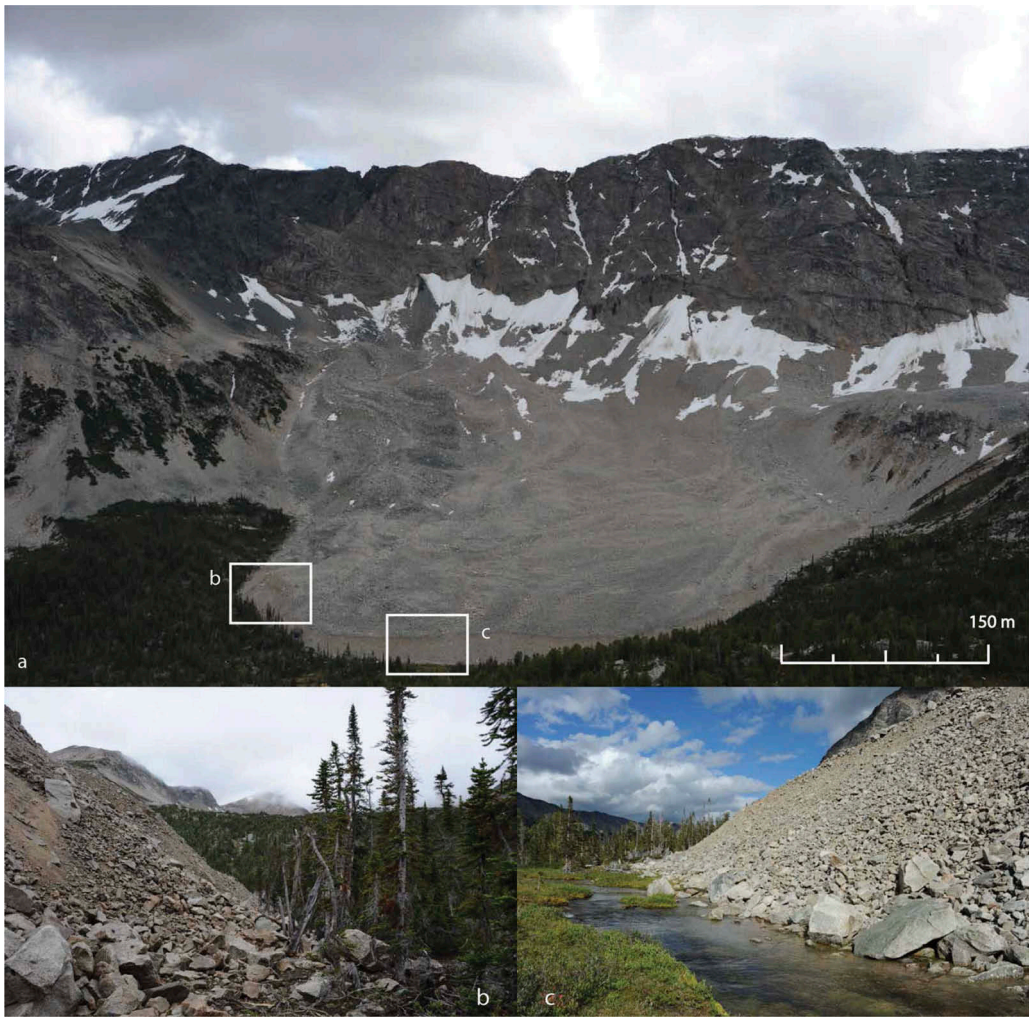

Figure 3. Hellraving rock glacier (#105). (a) North-facing rock wall and Hellraving rock glacier; (b) uppermost collection of sampled trees partially buried in the rock glacier toe debris; and (c) rock glacier toe and surrounding ponded area. Both smaller images were taken facing downslope.

Minimum kill dates were assigned by cross-dating the samples to existent master tree-ring chronologies. Subalpine fir samples were cross-dated to a chronology collected by Starheim, Smith, and Prowse (2013) at Jacobsen Glacier in the nearby Monarch Icefield area (AD 1533–2009). Whitebark pine samples were cross-dated to a tree-ring chronology from Siva Glacier (AD 1189–2000) constructed by Larocque and Smith (2005a; Table 1). The cross-dating was verified using COFECHA (Grissino-Mayer 2001; Holmes 1983), and the age of the outermost ring was assigned using the COFECHA master chronology.

Results

Inventory and distribution

A total of 165 intact rock glaciers were identified in the study area (Figure 6, Table 2) with an indeterminate number likely overlooked because of topographic shading or poor image quality. Rock glaciers appeared evenly distributed within the intrusive, sedimentary, and volcanic rocks that characterize the southeastern front ranges of the Coast Mountains (Figure 6b, Table 3). Rock glacier distribution was bounded by the Yalakom and Fraser faults to the east and plutons to the west. Rock glaciers have formed within the volcanic, marine, and sedimentary rocks of the Bridge River, Cadwallader, Methow, and Overlap terranes. Rock glaciers also formed within localized granitodioritic intrusives associated with the Post Accretionary terrane along the border between the southeast and southwest Coast Mountains.

In the study area rock glaciers occupy predominately north-facing (NW, N, NE) slopes (Figure 7). Glacier-derived rock glaciers display the broadest range of slope aspects, while talus-derived rock glaciers were primarily

Figure 4. Partially buried trunks and sheared stumps found in the frontal debris of Hellraving rock glacier: (a) sample HRG06 and (b) samples HRG14 (left) and HRG15 (right).

restricted to north-facing slopes (Figure 7). The mean elevations for glacier-derived features and talus-derived features are similar (2,100 ±50 m and 2,090 ±50 m, respectively; Table 4). Rock glaciers are generally located at sites with MAAT values of −1°C and MAP values of 1,250 mm/yr (Table 4). Despite some variation in the elevation or environmental conditions between categories (Table 4), the results of pairwise comparisons indicate that these differences are statistically insignificant (Table 5). No evidence was found to support a systematic difference in the altitudinal or environmental variables across the rock glacier categories.

The relationship between MAAT and elevation for glaciers and treeline was used to estimate the −3°C and 0°C isotherms, respectively (r = −0.87 for both; Figure 8). Because intact rock glaciers occur between the lower altitudinal boundary of glaciers and the upper extent of treeline (Figure 9, Figure 10), their distribution was largely bounded by the estimated −3°C isotherm (2,400 m) and the 0°C isotherm (1,800 m).

Dendrogeomorphology at Hellraving rock glacier

The remains of erect and partially buried tree trunks found along the leading edge of Hellraving rock glacier were excavated in July 2014. The majority of trunks were traced to rooted stumps and boles found tipped over or broken in the direction of assumed rock glacier movement (Figures 3 and 4). A single whitebark pine bole (HRG16) was found pressed against the proximal face of a large lichen-covered boulder 5 m from the debris edge. Buried to an estimated depth of 3 m, this tree appears to have been overwhelmed as debris spilled from the rock glacier margin to surround the boulder.

Eleven cross sections were collected: ten subalpine fir trees were cross-dated to the Jacobsen Glacier chronology

Figure 5. Hellraving rock glacier: (a) oldest sample (HRG16; AD 1674) shown pressed up against the proximal face of a large boulder and (b) close-up view of the sample, person for scale.

Table 1. Characteristics of master tree-ring chronologies.

Statistic	Subalpine Fir[a]	Whitebark Pine[b]
Number of trees	9	27
Number of cores	19	48
Chronology interval	1533–2009	1189–2000
Mean series correlation[c]	0.571	0.493
Mean sensitivity	0.192	0.214
Autocorrelation	0.768	0.856

[a]Master subalpine fir chronology collected at Jacobsen Glacier (Starheim, Smith, and Prowse 2013).
[b]Master whitebark pine chronology collected at Siva Glacier (Larocque and Smith 2005a).
[c]Mean series correlation coefficients are significant at the 99 percent confidence interval for $r > 0.328$. This value is a measure of chronology reliability and is reduced by dating errors and individual tree-level influences on growth. The value of this statistic also varies for species and distribution (Grissino-Mayer 2001).

(Figure 11), and one whitebark pine sample was cross-dated to the Siva Glacier chronology (Figure 12). Younger samples were significantly correlated ($r > 0.328$) to their respective master chronology for the entire growth period. The oldest samples (HRG01, HRG14, HRG16) were significantly correlated to the master chronology during the past 100 years of growth (Table 6). Beyond this range, limited sample depth within the master chronologies prevented accurate cross-dating (Figures 11 and 12). Because impact wounds were not observed on the samples, we assume that the trees died shortly after burial was initiated.

Dendrogeomorphological evidence describing the frontal advance of Hellraving rock glacier is limited to the northern snout area, where the trees were progressively buried by spilled debris. Large boulders with lichen-covered undersides characterize the steep talus apron in this location, suggesting that surface transport down the toe and deposition at the snout perimeter were responsible for the frontal advance (Barsch 1996; Koning and Smith 1999; Wahrhaftig and Cox 1959). Estimated rates of down-valley movement in this section range from 0.9 to 1.7 cm/yr (average 1.3 cm/yr) during the AD 1674–2003 period. In contrast, there is no evidence to suggest that the eastern toe area has moved down valley within the past 150 years (HRG01-12; Figure 13).

Discussion

Regional trends in the southwestern Canadian Cordillera

Rock glaciers are abundant in the southeastern front ranges of the Coast Mountains from 50°10′ to 52°08′ N latitude, with several forms present within a limited

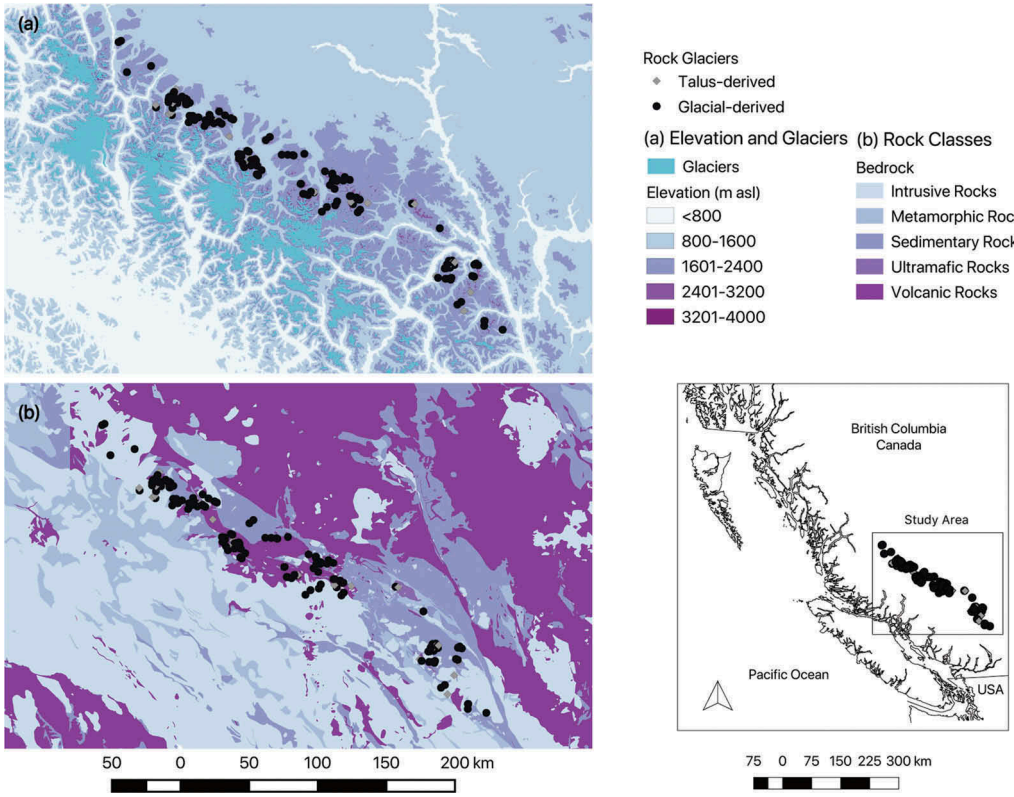

Figure 6. Map of the study area showing the location of the inventoried rock glaciers. The inset maps show the: (a) general terrain elevation of the study area and the location of prominent glaciers and icefields and (b) spatial position and extent of the major regional bedrock classes.

spatial area. Rock glaciers were observed originating from talus accumulated below steep headwalls, as well as in association with retreating glaciers. Rock glaciers were often seen extending from large hummocky moraines or directly from the debris-covered snouts of glaciers. Most rock glaciers have steep toe angles and appear to originate from fresh debris.

Contrary to findings in the southern Canadian Rocky Mountains, where rock glacier distribution is confined to the shales and quartzites of the Main Ranges, rock glacier distribution in the southeastern Coast Mountains appears to be consistent across several bedrock lithologies. While this finding is likely a product of the heterogeneous geology of the area and the coarse resolution of geologic maps (1:250,000; Massey et al. 2005), a close spatial association with the Yalakom fault system of the southern Chilcotin Ranges (Umhoefer and Schiarizza 1996) suggests that tectonic activity may influence headwall weathering rates and the production of talus. Where the large size of rock glaciers is not explained by local weathering rates and lithology, proximity to major faults known to trigger rock falls may account for high talus production (Bolch and Gorbunov 2014). Steep east-dipping faults, metamorphism, and volcanic arcs on the retro-wedge side of the bivergent Coast Mountain Range (Bustin et al. 2013; Mustard and van der Heyden 1997) warrant more investigation, yet are outside the scope of this research.

The distribution of intact rock glaciers at elevations above treeline (Figures 9 and 10) agrees with preliminary assessments of permafrost occurrence in the Coast Mountains. An average MAAT of −1°C for all rock glaciers (Table 4) corroborates regional estimates of the lower limit of permafrost along MAAT isotherms of −1°C (Brown and Péwé 1973; French and Slaymaker 1993) and colder than 0°C (Harris 1981; Rodenhuis et al. 2007; Table 7). The distribution also agrees with the general climatic boundaries of rock glacier development at high-elevation sites with below 0°C MAAT and moderate precipitation totals (<2,500 mm/yr; Brazier, Kirkbride, and Owens 1998; Haeberli 1985; Johnson, Thackray, and van Kirk 2007; Scotti et al. 2013).

In the study region, several of the rock glaciers included in the inventory were found at sites several kilometers up valley from the presumed terminal position of Younger Dryas valley glaciers (9390 ±40 BP; Grubb 2006). This maximum age, and that determined by Luckman and Crockett (1978; 9000 ±500 BP) for

Table 2. Rock glacier inventory for the Front Ranges study area, British Columbia.

Rock Glacier ID	Latitude	Longitude	Origin*	Aspect	Elevation (m)	MAAT °C** (1971–2000)	MAP mm/yr*** (1971–2000)	Rock Class
6	50.175419	−121.749534	G	NE	2,105	−0.7	865	Intrusive rocks
7	50.373081	−122.156613	G	NE	2,323	−2.1	1,079	Intrusive rocks
10	50.521211	−122.007336	T	NE	2,260	−1.7	1,017	Sedimentary rocks
11	50.520827	−122.00273	T	NE	2,179	−1.3	1,015	Sedimentary rocks
12	50.539016	−122.027788	G	NE	2,125	−1	995	Sedimentary rocks
13	50.53349	−122.010343	G	NW	2,079	−0.8	1,000	Intrusive rocks
14	50.606336	−121.96168	G	NW	1,848	0.5	980	Sedimentary rocks
15	50.614966	−121.994524	G	N	1,963	−0.1	900	Sedimentary rocks
16	50.618858	−121.981466	G	N	1,877	0.3	859	Sedimentary rocks
18	50.529705	−122.304763	G	N	2,118	−0.9	1,223	Intrusive rocks
20	50.550161	−122.401647	T	N	1,829	0.5	1,072	Intrusive rocks
21	50.538725	−122.381462	G	NW	2,188	−1.3	1,229	Sedimentary rocks
22	50.522131	−122.251104	G	NE	2,349	−2.2	1,173	Sedimentary rocks
23	50.533806	−122.243589	G	NE	2,164	−1.2	1,155	Sedimentary rocks
25	50.600505	−122.252385	G	NE	2,282	−1.9	1,181	Sedimentary rocks
26	50.630966	−122.212615	G	NE	2,126	−0.9	1,109	Sedimentary rocks
27	50.617122	−122.207504	G	E	2,248	−1.6	1,131	Sedimentary rocks
28	50.606048	−122.276794	G	N	2,261	−1.8	1,225	Sedimentary rocks
29	50.647269	−122.227317	G	N	2,047	−0.5	1,050	Sedimentary rocks
32	51.008102	−123.15361	G	N	2,061	−1.2	1,336	Intrusive rocks
33	51.04508	−123.225061	G	N	2,095	−1.5	1,452	Volcanic rocks
36	51.073244	−123.1531	G	N	2,219	−2	1,429	Sedimentary rocks
37	51.075975	−123.168184	G	NE	2,361	−2.5	1,464	Volcanic rocks
38	51.059688	−123.247225	T	NW	2,140	−1.8	1,439	Volcanic rocks
39	51.099469	−123.254887	G	NW	2,239	−2.3	1,448	Volcanic rocks
40	51.205447	−123.249795	G	NE	2,368	−2.9	1,433	Volcanic rocks
41	51.243372	−123.431025	G	NE	2,401	−2.9	1,463	Intrusive rocks
42	51.386017	−123.714918	G	NE	2,303	−2.2	1,318	Volcanic rocks
45	51.150155	−123.410851	G	NE	2,218	−1.9	1,425	Volcanic rocks
46	51.202023	−123.317247	G	S	2,438	−3.1	1,501	Sedimentary rocks
47	51.131506	−123.628737	G	NE	2,136	−1.4	1,371	Volcanic rocks
48	51.134327	−123.62036	T	N	2,042	−0.9	1,310	Volcanic rocks
49	51.137028	−123.6598	G	N	2,199	−1.7	1,421	Volcanic rocks
50	51.190475	−123.759492	G	N	2,106	−1.3	1,436	Volcanic rocks
51	51.190421	−123.763906	G	N	2,076	−1.2	1,443	Volcanic rocks
52	51.483008	−124.114532	G	NW	1,978	−0.6	937	Sedimentary rocks
53	51.416418	−124.313075	G	NE	1,972	−0.6	906	Volcanic rocks
54	51.373069	−124.290941	T	N	2,199	−1.8	1,022	Volcanic rocks
55	51.354376	−124.274765	G	NW	2,025	−0.9	1,001	Volcanic rocks
56	50.635029	−122.256061	G	NE	2,006	−0.4	1,168	Sedimentary rocks
57	50.645706	−122.260028	G	N	2,072	−0.7	1,099	Sedimentary rocks
58	50.631222	−122.234018	T	NW	2,294	−1.9	1,163	Sedimentary rocks
59	50.598356	−122.292211	G	NE	2,269	−1.8	1,223	Sedimentary rocks
60	50.607802	−122.275826	T	NW	2,239	−1.6	1,229	Sedimentary rocks
61	50.626162	−122.281938	T	NW	2,225	−1.6	1,206	Intrusive rocks
62	50.624339	−122.280117	G	NW	2,294	−2	1,216	Intrusive rocks
63	50.629341	−122.209323	G	NE	2,096	−0.8	1,095	Sedimentary rocks
64	50.63438	−122.198972	T	N	1,843	0.6	1,013	Sedimentary rocks
66	50.433633	−122.055525	T	NW	2,138	−1.2	983	Intrusive rocks
68	50.612318	−122.000363	G	N	2,021	−0.4	906	Sedimentary rocks
69	51.049368	−123.072936	T	N	2,088	−1.2	1,352	Sedimentary rocks
71	51.073058	−123.159847	G	N	2,282	−2.2	1,443	Volcanic rocks
72	51.251019	−123.428121	G	NE	2,282	−2.3	1,420	Intrusive rocks
73	51.26715	−123.505111	G	N	2,228	−1.8	1,450	Volcanic rocks
74	51.201138	−123.429216	G	NW	2,149	−1.6	1,489	Sedimentary rocks
76	51.225112	−123.300504	G	N	2,220	−2.3	1,454	Sedimentary rocks
77	51.410508	−124.296703	G	N	2,034	−0.9	927	Volcanic rocks

(*Continued*)

Table 2. (Continued).

Rock Glacier ID	Latitude	Longitude	Origin*	Aspect	Elevation (m)	MAAT °C** (1971–2000)	MAP mm/yr*** (1971–2000)	Rock Class
78	51.333753	−124.328168	T	NW	1,864	−0.3	973	Volcanic rocks
79	51.321219	−124.329791	T	W	1,907	−0.5	1,016	Volcanic rocks
80	51.394227	−124.378666	G	NE	2,094	−1.3	908	Sedimentary rocks
82	51.513475	−124.49853	T	N	2,015	−0.9	988	Volcanic rocks
86	51.635886	−124.679723	T	E/NE	2,120	−1.7	1,393	Sedimentary rocks
87	51.627741	−124.681722	G	NE	2,194	−2	1,478	Sedimentary rocks
89	51.656555	−124.700919	G	N	2,101	−1.5	1,446	Sedimentary rocks
91	51.619558	−124.870255	T	E/NE	2,344	−2.8	2,075	Intrusive rocks
98	51.595827	−124.561841	T	N	1,952	−0.9	1,164	Volcanic rocks
99	51.597255	−124.575341	G	NE	2,105	−1.6	1,227	Volcanic rocks
100	51.617722	−124.632294	T	N	2,112	−1.6	1,172	Volcanic rocks
101	51.584433	−124.756586	G	NW	1,929	−0.8	1,516	Metamorphic rocks
102	51.658797	−125.098686	G	NE	1,806	−0.2	1,164	Intrusive rocks
103	51.666102	−125.129041	T	N	2,159	−1.9	1,368	Intrusive rocks
104	51.673658	−125.103825	T	NE	1,958	−0.9	1,252	Intrusive rocks
105	51.705	−125.0911	G	NW	1,799	−0.2	1,214	Intrusive rocks
106	51.710322	−125.265052	G	W	2,038	−1.3	1,765	Intrusive rocks
107	51.725998	−125.268275	T	SW	2,175	−1.9	1,762	Intrusive rocks
109	51.737491	−124.908016	G	NE	2,125	−1.6	1,349	Intrusive rocks
111	51.759074	−124.937553	G	NE	1,991	−1.3	1,281	Metamorphic rocks
112	51.778683	−124.988355	G	N	1,960	−1.1	1,365	Metamorphic rocks
113	51.759786	−125.003286	G	NW	2,067	−1.7	1,381	Intrusive rocks
114	51.759736	−125.012622	T	N	2,054	−1.6	1,280	Intrusive rocks
115	51.736925	−125.020177	T	N	1,916	−0.7	1,282	Intrusive rocks
116	51.737316	−125.038477	G	NW	1,977	−1	1,229	Metamorphic rocks
117	51.737377	−125.090666	T	N	2,110	−1.8	1,325	Intrusive rocks
118	51.762872	−125.061016	G	NW	2,151	−2.1	1,280	Intrusive rocks
119	51.775511	−125.063783	G	NE	1,935	−1.1	1,347	Volcanic rocks
120	51.795993	−125.068718	T	N	2,207	−2.5	1,444	Volcanic rocks
121	51.795244	−125.077841	T	N	2,274	−2.8	1,458	Volcanic rocks
122	51.79563	−125.08265	G	NE	2,299	−2.9	1,472	Volcanic rocks
123	51.76843	−125.136975	T	NW	1,988	−1.4	1,262	Intrusive rocks
124	51.829519	−125.05255	T	N	1,884	−0.8	1,150	Sedimentary rocks
125	51.81	−125.072758	G	NE	2,328	−3.1	1,440	Volcanic rocks
126	51.942625	−125.570741	G	NE	1,854	−0.6	1,914	Intrusive rocks
143	50.52857	−122.27079	G	N	2,027	−0.5	1,187	Sedimentary rocks
144	51.355926	−124.262344	G	N	2,066	−1	988	Volcanic rocks
145	51.365933	−124.402236	G	NW	2,318	−2.6	1,276	Metamorphic rocks
146	51.396684	−124.406489	G	N	1,969	−0.6	901	Sedimentary rocks
147	51.370792	−124.385148	G	E	2,353	−2.8	1,242	Metamorphic rocks
148	51.381287	−124.374009	G	N	2,045	−1.1	952	Metamorphic rocks
149	51.380524	−124.385355	G	NE	2,230	−2.1	1,108	Metamorphic rocks
150	51.335419	−124.365377	G	E	1,873	−0.4	983	Metamorphic rocks
151	51.309639	−124.347599	G	N	2,136	−1.5	1,069	Metamorphic rocks
152	51.319524	−124.276679	G	E	2,319	−2.5	1,182	Volcanic rocks
153	51.340875	−124.225348	G	E	2,212	−1.9	971	Volcanic rocks
154	51.352197	−124.224267	G	N	2,110	−1.3	965	Sedimentary rocks
155	51.360337	−124.232731	G	NE	2,259	−2.2	984	Sedimentary rocks
156	51.31711	−124.211712	G	NE	2,044	−0.9	924	Volcanic rocks
157	51.287321	−124.167304	G	N	1,755	0.2	809	Volcanic rocks
158	51.260939	−124.209622	G	NE	2,111	−1.2	979	Volcanic rocks
159	51.253848	−124.205313	G	NE	2,007	−0.8	1,037	Volcanic rocks
160	51.261243	−124.219066	G	N	2,026	−0.9	917	Volcanic rocks
161	51.125043	−123.740312	G	N	2,070	−1.3	1,377	Sedimentary rocks
162	51.123484	−123.731892	G	N	2,274	−2.3	1,432	Sedimentary rocks
163	51.115832	−123.690912	G	N	2,158	−1.7	1,470	Intrusive rocks
164	51.003863	−123.55213	G	N	2,036	−1	1,284	Intrusive rocks

(*Continued*)

Table 2. (Continued).

Rock Glacier ID	Latitude	Longitude	Origin*	Aspect	Elevation (m)	MAAT °C** (1971–2000)	MAP mm/yr*** (1971–2000)	Rock Class
165	51.033004	−123.498343	G	NW	2,072	−1.2	1,396	Intrusive rocks
166	51.042033	−123.410865	G	N	1,974	−1.3	1,387	Intrusive rocks
167	51.067693	−123.389149	G	W	1,936	−1	1,351	Intrusive rocks
168	51.175526	−123.457953	G	N	2,201	−1.8	1,401	Volcanic rocks
169	51.227956	−123.419514	G	NE	2,239	−2.2	1,506	Intrusive rocks
170	51.213897	−123.382515	G	NE	2,247	−2.2	1,382	Intrusive rocks
171	51.201678	−123.384648	G	NE	2,223	−2.1	1,417	Intrusive rocks
172	51.099578	−123.241908	G	W	2,379	−2.6	1,489	Volcanic rocks
173	51.088354	−123.186754	G	E	2,259	−2.2	1,490	Intrusive rocks
175	50.991061	−123.179059	G	NE	2,102	−1.4	1,412	Intrusive rocks
176	51.032517	−122.611649	G	NE	2,133	−1.2	1,268	ultramafic rocks
177	51.027508	−122.585858	T	W	2,283	−1.9	1,310	ultramafic rocks
184	50.861835	−122.336972	G	N	2,051	−0.5	1,105	Intrusive rocks
185	50.597924	−122.307167	G	N	2,250	−1.7	1,217	Sedimentary rocks
186	50.60055	−122.286553	G	N	2,346	−2.2	1,221	Sedimentary rocks
187	50.356731	−122.197028	G	N	2,053	−0.5	1,074	Intrusive rocks
188	50.311627	−122.134445	T	N	1,986	−0.3	989	Intrusive rocks
189	50.208104	−121.935411	G	N	2,091	−0.8	989	Intrusive rocks
190	50.240663	−121.927898	G	N	2,065	−0.6	912	Intrusive rocks
191	50.240934	−121.931587	G	N	2,109	−0.8	925	Intrusive rocks
193	51.37669	−123.826231	G	N	2,141	−1.5	1,387	Volcanic rocks
194	51.383036	−123.889976	G	NW	1,878	−0.3	1,179	Volcanic rocks
195	51.384695	−123.951952	G	NW	2,005	−0.7	1,030	Sedimentary rocks
196	51.623369	−124.452352	G	NE	1,992	−0.9	886	Intrusive rocks
197	51.63188	−124.476095	G	N	2,083	−1.4	1,201	Sedimentary rocks
198	51.65162	−124.5387	G	N	2,146	−1.9	1,181	Intrusive rocks
199	51.678009	−124.599334	G	N	2,198	−2.1	1,171	Intrusive rocks
200	51.610604	−124.603322	G	N	1,982	−1	1,197	Volcanic rocks
201	51.608616	−124.607021	G	N	2,000	−1.1	1,222	Volcanic rocks
202	51.600623	−124.658405	G	N	1,958	−0.9	1,388	Sedimentary rocks
203	51.622205	−124.74573	G	N	2,002	−1	1,256	Sedimentary rocks
204	51.641246	−124.818764	G	E	1,902	−0.6	1,418	Metamorphic rocks
205	51.651958	−124.878917	G	N	2,243	−2.2	1,745	Metamorphic rocks
206	51.652829	−124.91174	G	NW	1,401	1.7	932	Sedimentary rocks
207	51.610089	−124.922501	G	NW	1,896	−0.4	1,688	Metamorphic rocks
208	51.727332	−124.940932	G	N	2,047	−1.4	1,419	Intrusive rocks
209	51.727999	−124.94847	G	N	2,013	−1.2	1,416	Intrusive rocks
210	51.734762	−124.932981	G	N	2,010	−1.1	1,386	Metamorphic rocks
211	51.765796	−124.952287	G	N	2,007	−1.4	1,437	Metamorphic rocks
212	51.772756	−124.98926	G	N	2,217	−2.5	1,513	Metamorphic rocks
213	51.777548	−125.124112	G	N	1,955	−1.3	1,265	Volcanic rocks
214	51.757402	−125.132241	G	NW	2,094	−2	1,333	Intrusive rocks
215	51.743552	−125.133068	G	NW	2,146	−2	1,323	Intrusive rocks
217	51.981489	−125.313304	G	N	1,991	−1.3	1,874	Intrusive rocks
218	52.139517	−125.657863	G	NW	1,906	−0.8	2,113	Intrusive rocks
219	52.148027	−125.631995	G	N	1,990	−1.2	2,095	Intrusive rocks
226	51.503057	−124.072139	G	NE	2,009	−0.8	878	Sedimentary rocks
227	51.624839	−124.859507	G	NE	2,217	−2.1	2,113	Intrusive rocks
228	51.742597	−124.948544	G	E	2,109	−1.7	1,456	Metamorphic rocks
230	51.380188	−123.835641	G	NE	2,081	−1.2	1,407	Volcanic rocks
232	51.607242	−124.725755	G	NW	2,223	−2.2	1,592	Sedimentary rocks

*G = glacier-derived rock glacier; T = talus-derived rock glacier.
**Mean Annual Air Temperature.
***Mean Annual Precipitation.

Table 3. Distribution of rock glaciers across bedrock classes attained from the digital Geological Map of British Columbia (Massey et al. 2005).

Rock Classes	Glacier-derived	Talus-derived	Total Count
Intrusive	41	12	53
Metamorphic	17	0	17
Sedimentary	40	8	48
Ultramafic	1	1	2
Volcanic	35	10	45

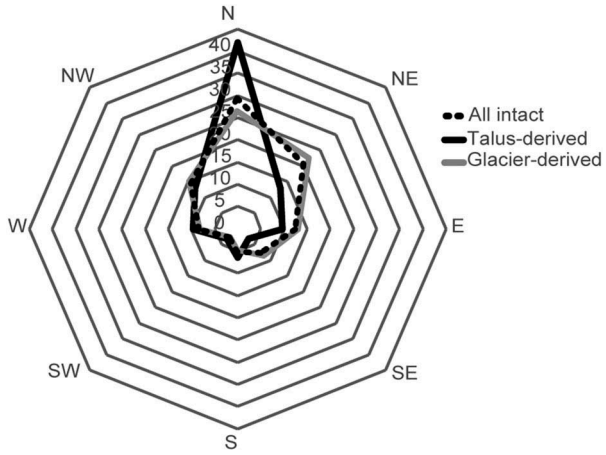

Figure 7. Relative abundance of slope aspects for all, glacier-derived, and talus-derived rock glaciers.

rock glaciers in the southern Canadian Rocky Mountains, suggests that most rock glaciers in the Canadian Cordillera are likely of Holocene age. Despite reports of up to seven Holocene glacier advances in the region (Menounos et al. 2009; Mood and Smith 2015), pre-LIA moraines are largely absent in the study area and many rock glaciers were found distal to inferred LIA terminus positions. These permafrost landforms are large, well developed, and unlikely to have been produced by LIA climates alone. Complex rock glacier landforms with apparently older tongues, partially overwhelmed by unweathered rock debris, can be found throughout the study area. Their presence could explain the lack of relict rock glaciers included within the inventory. Many permafrost landforms in the front ranges are, therefore, assumed to predate the LIA and signify the presence of periglacial activity influenced by permafrost climates during the Holocene. Unlike the findings of some rock glacier inventories, a clear altitudinal boundary between intact and relict forms is not present in this area, and the complex relationship between Holocene climate variability and rock glacier activity warrants further investigation.

Glacier-derived rock glaciers display a broader distribution in aspect orientation. While the majority face to the north-northeast, between 10 percent and 15 percent of these rock glaciers occupy east- and west-facing slopes (Figure 7). This finding suggests that topographic shading is not the dominant control of intact glacier-derived forms, as is evident with talus-derived rock glaciers, and that local conditions related to glacial dynamics are important for their distribution. Retreating glaciers lose energy through meltwater runoff, sometimes resulting in cold ablation areas with permafrost below the equilibrium line (Etzelmuller and Hagen 2005; Kneisel and Kaab 2007; Lilleøren et al. 2013b). This outcome, in combination with the high sediment supply of debris-covered glaciers (Kirkbride 2011), could explain a proglacial environment that is highly conducive to permafrost formation in the Front Ranges. The dominance of glacier-derived rock glaciers is consistent with other coastal-proximate studies, where frequent interaction between surface ice and permafrost conditions results in composite ice-debris features of both periglacial and glacial origin (Berthling 2011; Lilleøren et al. 2013a; Ribolini and Fabre 2006). In the European Alps and the Chilean Andes, active debris-ice features proximal to retreating glaciers indicate that a transition is occurring from glacial to periglacial processes under the contemporary climate (Monnier and Kinnard 2015; Seppi et al. 2015). Rock glaciers respond slower than glaciers to climatic variability because of the cooling and insulating effects of a thick debris cover (Janke et al. 2013; Kirkbride 2011). A large proportion of the glacier-derived features included within this inventory were observed

Table 4. Summary of the environmental variables collected within the rock glacier inventory.

Landform Category	Number of Landforms	Elevation (m)	MAAT °C (1971–2000)	MAP mm/yr (1971–2000)
All intact rock glaciers	165	2,102 (152)	−1.2 (0.8)	1,258 (245)
Glacier-derived	134	2,104 (153)	−1.2 (0.8)	1,264 (249)
Talus-derived	31	2,090 (147)	−1.1 (0.8)	1,236 (229)

MAAT = mean annual air temperature; MAP = mean annual precipitation; standard deviation in brackets.

Table 5. Results of the pairwise comparisons of environmental variables by rock glacier category.

	Intact
Variable	Glacier-derived vs. talus-derived
Elevation (m)	
Chi-square	0.172
Significance	0.678
MAAT (°C)	
Chi-square	0.013
Significance	0.909
MAP (mm/yr)	
Chi-square	0.831
Significance	0.362

MAAT = mean annual air temperature; MAP = mean annual precipitation.

originating from the debris-covered termini of retreating glaciers, suggesting that a similar transition is occurring in the Coast Mountains. Environmental conditions in the front ranges are, therefore, assumed to be presently conducive to periglacial activity yet are unable to support positive glacial mass-balance conditions. This finding further suggests that periglacial activity in this region may have persisted throughout interstadial periods of glacial retreat during the Holocene.

Movement at Hellraving rock glacier

The observed rates of frontal movement at Hellraving rock glacier are comparable to those described at sites in the Canadian Rocky Mountains, where similar investigations describe rates of frontal advance at two rock glaciers ranging from 1.2 to 1.6 cm/yr throughout the past several centuries (Bachrach et al. 2004; Carter et al. 1999). Comparable rates of contemporary frontal advance averaging 1.6 cm/yr were established by geodetic surveys at King's Throne rock glacier in the Front Ranges of the Canadian Rocky Mountains (Koning and Smith 1999).

The rate of frontal advance established for Hellraving rock glacier is comparable to that recorded at other sites in North America and is similar to those reported for rock glaciers located in Central Asia, Greenland, and Svalbard (Table 8). Unlike the situation at many locations in the European Alps, where warming permafrost has accelerated rock glacier advance since the 1990s to several meters per year (Bodin et al. 2009; Delaloye et al. 2008, 2013; Ikeda, Matsuoka, and Kääb 2008; Roer et al. 2008), there was no indication of recent changes in the rate of frontal advance at Hellraving rock glacier. In this regard the behavior of Hellraving rock glacier is similar to that of rock glaciers in Colorado, where the rock glaciers are acclimatized to the present-day climate and do not display significant increases in activity during the past sixty years (Janke 2005).

Conclusion

This study is the first to report on the presence of intact and active rock glaciers within the southeastern front ranges of the British Columbia Coast Mountains. All the rock glaciers surveyed are located at elevations between that of cirque glaciers in the region (average 2,400 ±50 m a.s.l.) and the local treeline (average 1,900 ±50 m a.s.l.). The research indicates that rock glacier distribution in the southeastern front ranges can be partly explained by topography and Holocene climates. Statistical rock glacier distribution models, with variables related to surface

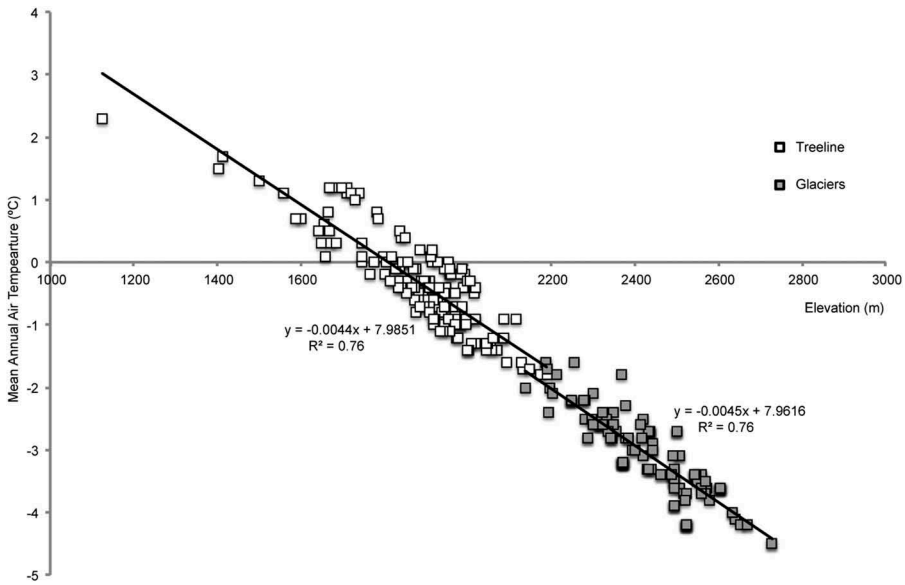

Figure 8. The relationship between mean annual air temperature and elevation used to estimate the 0°C and −3°C isotherms.

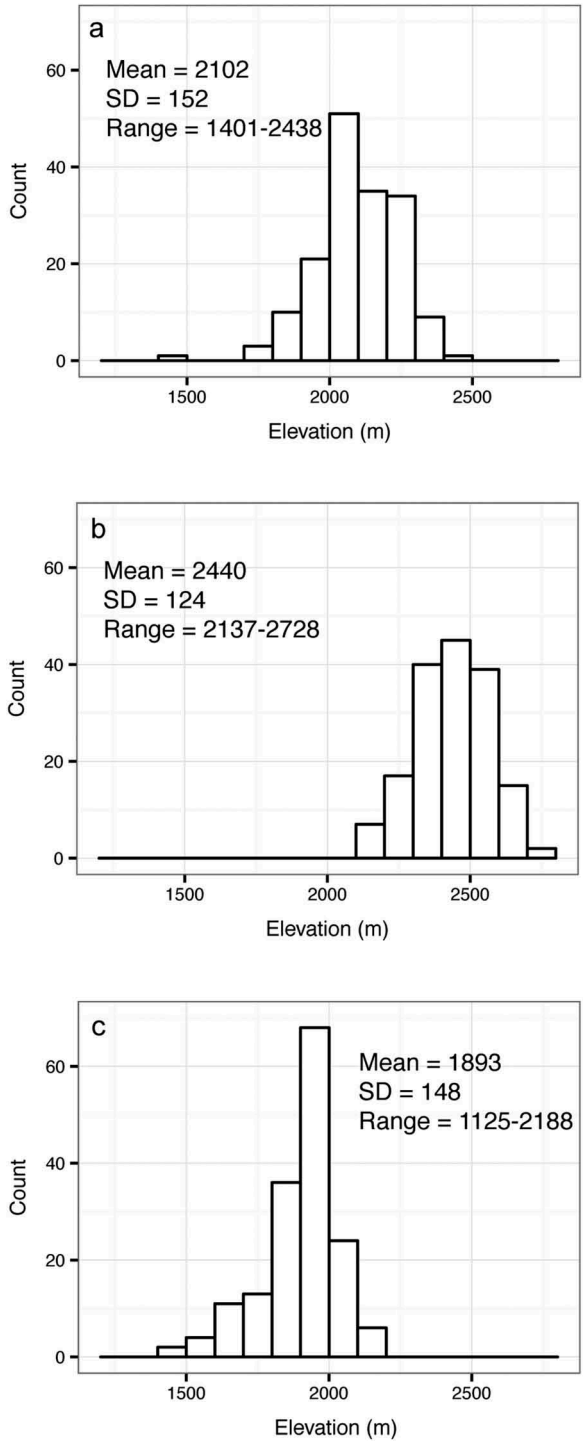

Figure 9. Regional elevation histograms for (a) intact rock glaciers, (b) glaciers, and (c) treeline. Each column represents 100 m in elevation.

characteristics, snow accumulation, and topography (i.e., Brenning, Grasser, and Friend 2007; Brenning and Trombotto 2006; Esper Angillieri 2010; Johnson, Thackray, and van Kirk 2007), as well as ground temperature data, will be necessary to provide a detailed distribution of permafrost conditions (cf. Bonnaventure et al. 2012) in the Coast Mountains.

The estimated rate of frontal advance (1.3 cm/yr) for one rock glacier in the study area appears to have remained constant since AD 1674, even as rising regional air temperatures promoted glacial retreat and downwasting from LIA terminal positions (Bolch, Menounos, and Wheate 2010; Larocque and Smith 2003; Schiefer, Menounos, and Wheate 2007). These

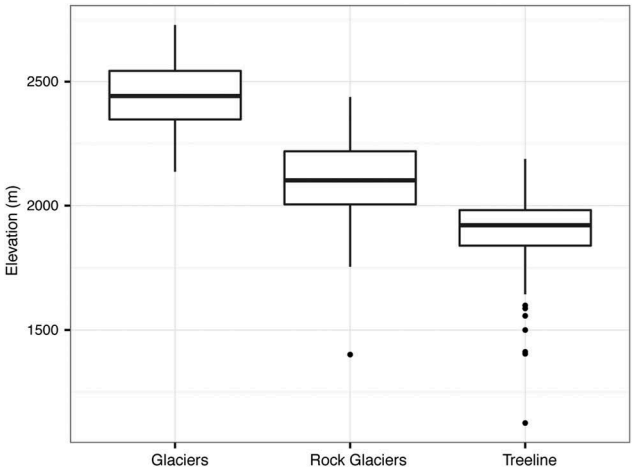

Figure 10. Boxplots indicate the elevation of inventoried intact rock glaciers as compared to glaciers and treeline. Outliers are shown as dots.

results are consistent with similar studies in the Canadian Rocky Mountains and support the observation of Janke (2005) that climatic variability in North America has not caused the same marked change in rock glacier dynamics as witnessed in the European Alps (Delaloye et al. 2013; Roer et al. 2008). If air temperatures on the lee side of the British Columbia Coast Mountains continue to rise (Dawson, Werner, and Murdock 2008), however, the geomorphic activity of Hellraving rock glacier and other similarly positioned rock glaciers may soon fundamentally change.

The abundance of intact rock glaciers originating from the moraines and from the heavily debris-laden tongues of small alpine glaciers suggests that glacial and periglacial systems are highly interrelated in the Coast Mountains. Because air temperatures are predicted to continue rising in the study area (Dawson, Werner, and

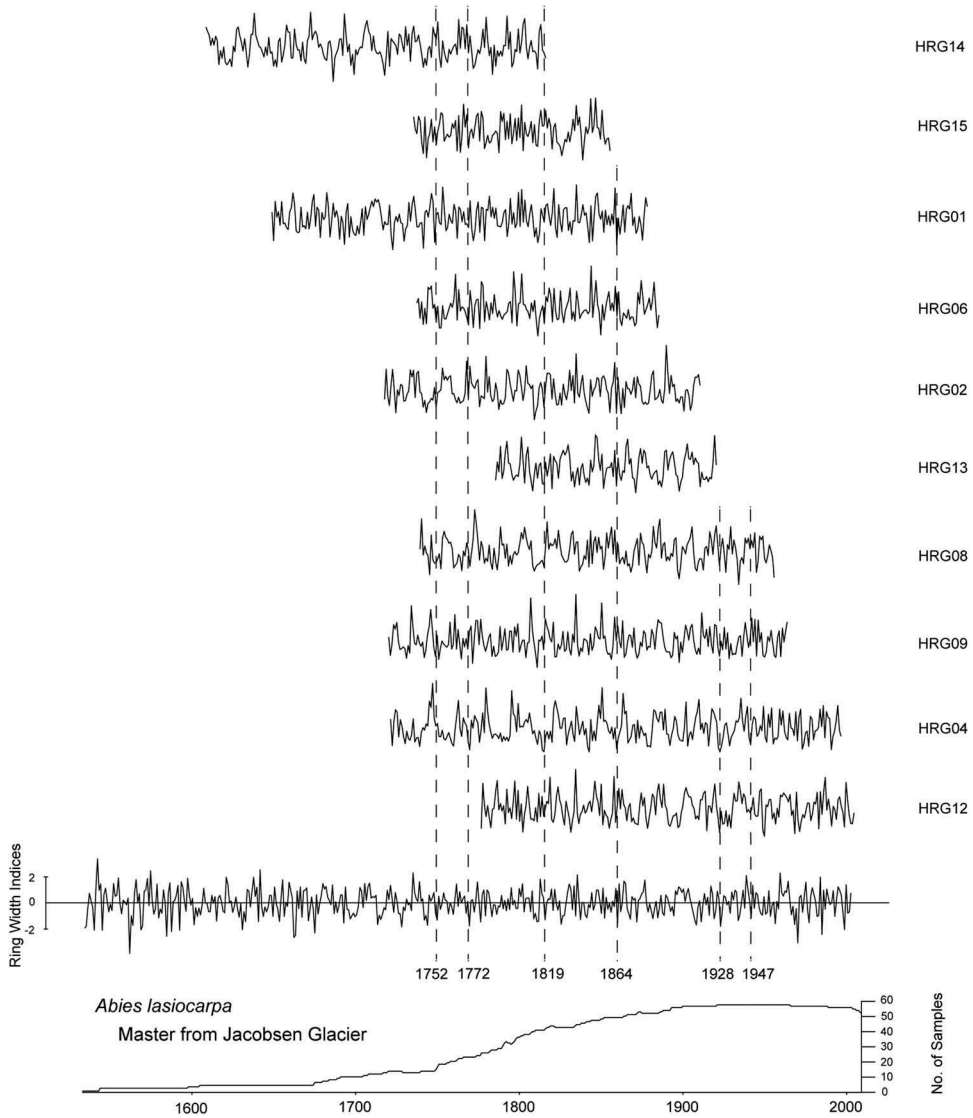

Figure 11. Subalpine fir samples from Hellraving rock glacier visually cross-dated into the living subalpine fir master chronology from Jacobsen Glacier. Marker years, indicated by the dashed lines, were used to visually cross-date before verifying in COFECHA.

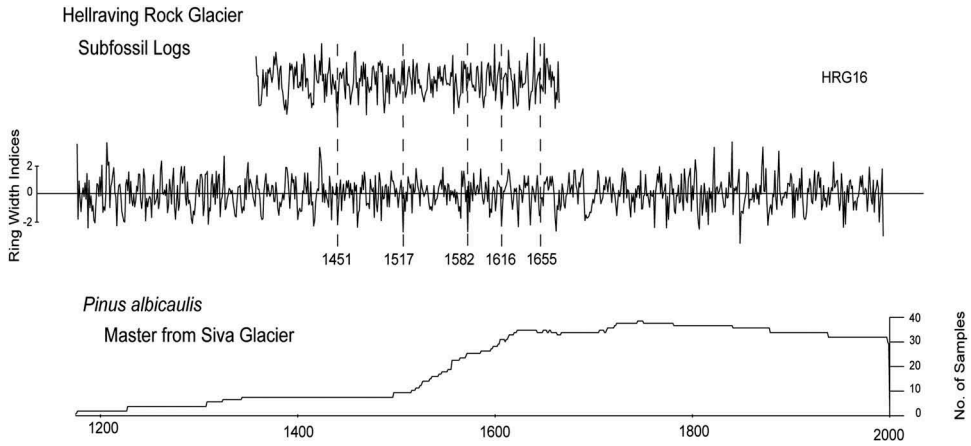

Figure 12. Whitebark pine sample from Hellraving rock glacier visually cross-dated to the living whitebark pine master chronology from Siva Glacier. Marker years, indicated by the dashed lines, were used to visually cross-date before verifying in COFECHA.

Table 6. Kill dates and estimates of Hellraving rock glacier advance rate.

Sample Number	Species[a]	Mean Correlation to Master Chronology[b]	Death Date (yr AD)	Distance Buried (m)	Rate of Movement (cm/yr)
HRG01	SAF	0.204 (0.48)[c]	1883	0	0
HRG02	SAF	0.371[c]	1916	0	0
HRG04	SAF	0.375[c]	2003	0	0
HRG06	SAF	0.546[c]	1890	1	0.8
HRG08	SAF	0.359[c]	1962	0	0
HRG09	SAF	0.446[c]	1970	0	0
HRG12	SAF	0.432[c]	2013	0	0
HRG13	SAF	0.377[c]	1926	1.5	1.7
HRG14	SAF	0.205 (0.44)[c]	1820	1.75	0.9
HRG15	SAF	0.547[c]	1860	2	1.3
HRG16	WBP	0.307 (0.37)[d]	1674	5	1.5

[a]SAF = subalpine fir (*Abies lasiocarpa*); WBP = whitebark pine (*Pinus albicaulis*).
[b]This value is the mean correlation between the master chronology and the undated sample. Correlation coefficients are significant at the 99 percent confidence interval for $r > 0.328$. For samples that are insignificantly correlated for the entire growth period, the correlation value for the past 100 years of growth is provided in brackets.
[c]Master subalpine fir chronology collected at Jacobsen Glacier (Starheim, Smith, and Prowse 2013).
[d]Master whitebark pine chronology collected at Siva Glacier (Larocque and Smith 2005a).

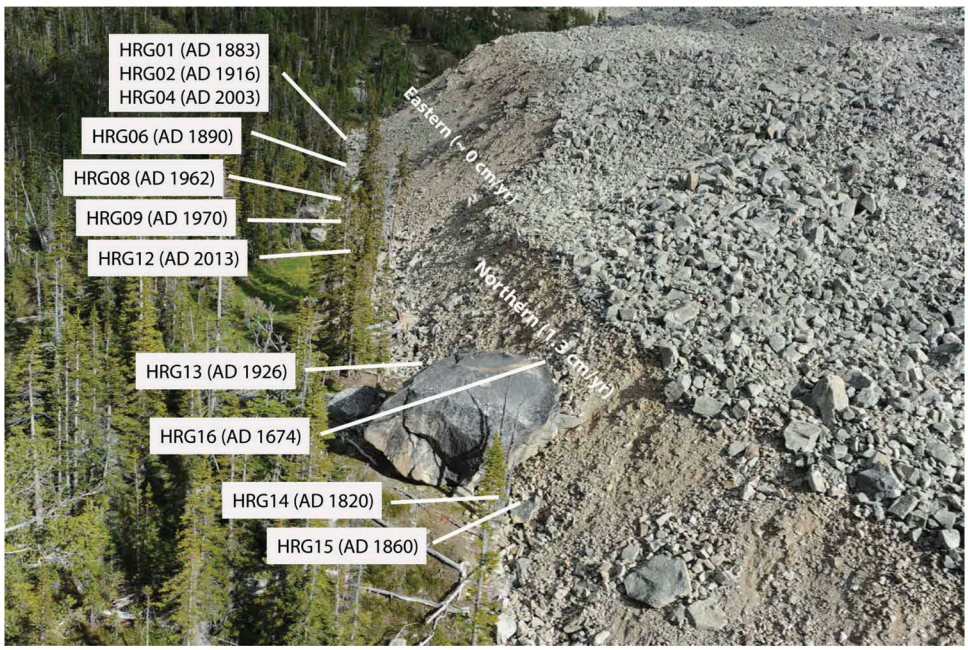

Figure 13. Sample numbers and kill dates for trees sampled from the toe debris of Hellraving rock glacier. The northern and eastern sections of the terminus are also indicated along with the average advance rates.

Table 7. Previous estimates of permafrost in the front ranges of the Coast Mountains.

Author	Scope of Research	Permafrost Attributes in the Southern Coast Mountains	Methodology
Distribution of permafrost in North America (Brown and Péwé 1973)	North America	Map: Large extent of eastern portion indicated as "permafrost areas at high altitude in cordillera south of [discontinuous] permafrost limit"	Review of permafrost research in North America; adapted "Permafrost in Canada" map (Brown 1967)
National Atlas of Canada 5th edition: Permafrost (Heginbottom, Dubreuil, and Harker 1995)	Canada	Map: Eastern extent contains "isolated patches" (0–10% permafrost)	Contoured ground temperature measurements (Heginbottom 2002)
Climate Overview (Rodenhuis et al. 2007)	British Columbia	Map: Large extent of eastern portion with MAAT below 0°C isotherm, indicative of frozen terrain	Annual mean temperature (Canadian Climate Normals 1961–1990) interpolated using PRISM (4 km; Wang et al. 2006)
Canada's Cold Environments (French and Slaymaker 1993)	"Canada's Cold Land Mass"	Section of alpine permafrost exists in the southern Coast Mountains; southern limit of discontinuous permafrost coincides with MAAT of −1°C	Map adapted from Associate Committee on Geotechnical Research (1988)
	"Cold Mountains of Western Canada"	Permafrost restricted to high mountain altitudes greater than 2,300 m; periglacial activity occurs below treeline (~1,650 m) west of the continental divide	Lowest visible indicator of permafrost/periglacial activity in Garibaldi National Park

Table 8. Published rates of rock glacier frontal advance. Based in part on Roer (2005) and Burger, Degenhardt, and Giardino (1999).

Region	Location	Frontal Advance (m/yr)	Measurement Period	Method	Reference
Central Asia	Kazakhstan, Tian Shan, Zailijskiy Alatau, Gorodetskiy	0.4–0.90.90.7	1923–1946 1946–1960 1960–1977	?	Gorbunov (1983)
	Kazakhstan, Northern Tien Shan and Djungar Ala Tau	0.6–0.9	?	?	Gorbunov, Titkov, and Polyakov (1992) from Burger, Degenhardt, and Giardino (1999)
Greenland	Greenland, Disko Island, Mellemfjord	0.1	1984–1985	?	Humlum (1996)
Svalbard	Norway, Svalbard, Hiorthfjellet	0.03	1994–2002	Photogrammetry and terrestrial geodetic survey	Ødegard et al. (2003)
European Alps	Austria, Stubai Alps, Reichenkar	0.64[a]	1954–1990	Photogrammetry	Krainer and Mostler (2000)
	Austria, Stubai Alps, Reichenkar	3	1990–2003	Photogrammetry	Hausmann et al. (2007)
	Austria, Ötztal Alps, Innere Ölgrube	0.60[a]	1969–2000	Aerial photography	Berger, Krainer, and Mostler (2004)
	Austria, Ötztal Alps, Äusseres Hochebenkar	3–4	1936–1953	Terrestrial photogrammetry	Pillewizer (1957) from Roer (2005)
	Austria, Ötztal Alps, Äusseres Hochebenkar	2.4–2.7 1.1 5.0	1936–1997 1977–1997 1953–1969	Terrestrial geodetic survey	Schneider and Schneider (2001) from Roer (2005)
	France, French Alps, Laurichard	0.3	1994–2002	Terrestrial geodetic survey	Francou and Reynaud (1992)
	France, French Alps, Laurichard	0.5[a] 0–0.6	1975–2005 2005–2006	Terrestrial LIDAR and photogrammetry	Bodin, Schoeneich, and Jaillet (2008)
	Switzerland, Grisons, Val Sassa Switzerland, Grisons, Val dell' Acqua	0.39 0.43	1921–1942	Painted line of rocks	Chaix (1943)
	Switzerland, Grisons, Murtèl Switzerland, Grisons, Muragl	0.01 0.05	1987–1996 1981–1994	Photogrammetry	Kääb (1997) from Roer (2005)
	Switzerland, Grisons, Muragl	0.17	1981–1994	Photogrammetry	Kääb and Kneisel (2006)
	Switzerland, Valais, Furggentälti	0.4	1960–1995	Photogrammetry	Krummenacher et al. (1998) from Roer (2005)
	Switzerland, Valais, Gruben	0.15	1970–1995	Photogrammetry	Kääb (1996) from Roer (2005)
	Switzerland, Valais, Grueol Switzerland, Valais, Furggwanghorn Switzerland, Valais, Petit-Vélan Switzerland, Valais, Tsaté-Moiry	2.30 1.55 2.50 4.00	1975–2001 1975–2001 1999–2005 1999–2005	Photogrammetry + terrestrial geodetic survey	Roer et al. (2008)

(*Continued*)

Table 8. (Continued).

Region	Location	Frontal Advance (m/yr)	Measurement Period	Method	Reference
North America	Canada, Rocky Mountains, Lake Louise, Wenkchemna	0.04–0.50	1904–1905	Painted line of rocks	Sherzer (1907)
	Canada, Rocky Mountains, Lake Louise, various rock glaciers	0.30–0.60	1947–1974	Aerial photography	Osborn (1975)
	Canada, Rocky Mountains, King's Throne	0.016[a]	1988–1996	Terrestrial geodetic survey	Koning and Smith (1999)
	Canada, Rocky Mountains, Hilda Creek	0.012[a]	1856–1997	Dendrogeomorphology	Carter et al. (1999)
	Canada, Rocky Mountains, Hilda	0.016[a]	1576–1999	Dendrogeomorphology	Bachrach et al. (2004)
	Canada, Yukon Territory, Slims River	0–0.20	1984–1986	Terrestrial geodetic survey	Blumstengel and Harris (1988)
	Canada, Coast Mountains, Hellraving	0.013[a]	1674–2014	Dendrogeomorphology	This study
	USA, Alaska Range, Clear Creek	0.48[a]	1949–1957	Painted line of rocks	Wahrhaftig and Cox (1959)
	USA, Absaroka Mountains, Galena Creek	0.03–0.14	1964–1966	Painted line of rocks	Potter (1972)
	USA, Sierra Nevada	0.1–0.2	1947–1972	Aerial photography	Clark et al. (1994a, 1994b)
	USA, Colorado Front Range	0.05–0.2	1961–1975	Painted line of rocks	White (1971, 1987)

? = No details.
[a]Averaged rate of frontal advance.
Photogrammetry = Aerial photogrammetry, unless specified.
Terrestrial geodetic survey = Survey using theodolite or total station.

Murdock 2008), the influence of disappearing glaciers on permafrost landforms downslope should be monitored. Rock glaciers can store significant amounts of freshwater during times of drought, and an understanding of their internal characteristics and behavior is important to future water security in this region (Rangecroft et al. 2014). The inventory presented here is the first step toward monitoring rock glacier dynamics under changing climate regimes in the mountain landscapes of southwestern British Columbia.

Acknowledgments

Research funding was provided by a Natural Sciences and Engineering Research Council of Canada (NSERC) Discovery Grant to Smith. We thank Øyvind Paasche and an anonymous reviewer for their thoughtful insights and suggestions for improvement on an earlier version of the manuscript. Special thanks are offered to Bryan Mood and Vikki St-Hilaire for their assistance in the field.

Disclosure statement

No potential conflict of interest was reported by the authors.

References

Associate Committee on Geotechnical Research. 1988. *Glossary of Permafrost and Related Ground-Ice Terms. Technical Memorandum*, Vol. 142. Ottawa, ON: National Research Council Canada.

Bachrach, T., K. Jakobsen, J. Kinney, P. Nishimura, A. Reyes, C. P. Laroque, and D. J. Smith. 2004. Dendrogeomorphological assessment of movement at Hilda rock glacier, Banff National Park, Canadian Rocky Mountains. *Geografiska Annaler* 84A:1–9.

Barsch, D. 1996. *Rockglaciers: Indicators for the Present and Former Geoecology in High Mountain Environments*. Heidelberg, Berlin: Springer-Verlag.

Berger, J., K. Krainer, and W. Mostler. 2004. Dynamics of an active rock glacier (Ötztal Alps, Austria). *Quaternary Research* 62:233–42.

Berthling, I. 2011. Beyond confusion: Rock glaciers as cryo-conditioned landforms. *Geomorphology* 131:98–106.

Blumstengel, W. K., and S. A. Harris. 1988. Observations on an active lobate rock glacier, Slims River Valley, St. Elias Range, Canada. In *Proceedings of the 5th International Conference on Permafrost*, ed. K. Senneset., Vol. 1, 689–94. Trondheim: Norway, Tapir Publishers.

Bodin, X., P. Schoeneich, and S. Jaillet. 2008. High-resolution DEM extraction from terrestrial LIDAR topometry and surface kinematics for the creeping alpine permafrost: The Laurichard rock glacier case study (Southern French Alps). *Proceedings of the Ninth International Conference on Permafrost*, D. L. Kane, and K. M. Hinkel, eds., Vol. 1, 137–42. Fairbanks: University of Alaska.

Bodin, X., E. Thibert, D. Fabre, A. Ribolini, P. Schoeneich, B. Francou, L. Reynaud, and M. Fort. 2009. Two decades of responses (1986–2006) to climate by the Laurichard rock glacier, French Alps. *Permafrost and Periglacial Processes* 20:331–44. Fairbanks: University of Alaska.

Boeckli, L., A. Brenning, S. Gruber, and J. Noetzli. 2012. Permafrost distribution in the European Alps:

Calculation and evaluation of an index map and summary statistics. *The Cryosphere* 6:807–20.

Bolch, T., and A. P. Gorbunov. 2014. Characteristics and Origin of Rock Glaciers in Northern Tien Shan (Kazakhstan/ Kyrgyzstan). *Permafrost and Periglacial Processes* 25:320–32.

Bolch, T., B. Menounos, and R. Wheate. 2010. Landsat-based inventory of glaciers in western Canada 1985 – 2005. *Remote Sensing of the Environment* 114:127–37.

Bonnaventure, P. P., A. G. Lewkowicz, M. Kremer, and M. C. Sawada. 2012. A permafrost probability model for the southern Yukon and northern British Columbia, Canada. *Permafrost and Periglacial Processes* 23:52–68.

Brazier, V., M. P. Kirkbride, and I. F. Owens. 1998. The relationship between climate and rock glacier distribution in the Ben Ohau Range, New Zealand. *Geografiska Annaler* 80A:193–207.

Brenning, A. 2005. Geomorphological, hydrological and climatic significance of rock glaciers in the Andes of Central Chile (33-35S). *Permafrost and Periglacial Processes* 16:231–40.

Brenning, A., M. Grasser, and D. A. Friend. 2007. Statistical estimation and generalized additive modeling of rock glacier distribution in the San Juan Mountains, Colorado, United States. *Journal of Geophysical Research* 112:1–10.

Brenning, A., and D. Trombotto. 2006. Logistic regression modeling of rock glacier and glacier distribution: Topographic and climatic controls in the semi-arid Andes. *Geomorphology* 81:141–54.

Brown, R. J. E., 1967: *Permafrost in Canada. Map* NRC *9769*. National Research Council of Canada, Division of Building Research, Ottawa, and Geological Survey of Canada Map 1246A.

Brown, R. J. E., and T. L. Péwé, 1973: Distribution of permafrost in North America and its relationship to the environment: A review, 1963-1973. In *Permafrost: North* American *Contribution [to The] Second International Conference*. Washington, DC:National Academy of Sciences.

Burger, K. C., J. J. Degenhardt Jr, and J. R. Giardino. 1999. Engineering geomorphology of rock glaciers. *Geomorphology* 31:93–132.

Bustin, A. M. M., R. M. Clowes, J. W. H. Monger, and J. M. Journeay. 2013. The southern Coast Mountains, British Columbia: New interpretations from geological, seismic reflection, and gravity data. *Canadian Journal of Earth Sciences* 50:1033–50.

Carter, R., S. LeRoy, T. Nelson, C. P. Laroque, and D. J. Smith. 1999. Dendroglaciological investigations at Hilda Creek rock glacier, Banff National Park, Canadian Rocky Mountains. *Géographie Physique Et Quaternaire* 53:365–71.

Chaix, A. 1943. Les coulées des blocs du Parc National Suisse: Nouvelles mesures et comparison avec les "rock streams" de la Sierra Nevade de Californie. *Le Globe* 82:121–28.

Clark, D. H., M. M. Clark, and A. R. Gillespie. 1994a. Debris-covered glaciers in the Sierra Nevada, California, and their implications for snowline reconstruction. *Quaternary Research* 41:139–53.

Clark, D. H., M. M. Clark, and A. R. Gillespie. 1994b. Reply to comment by M. Jakob on debris-covered glaciers in the Sierra Nevada, California, and their implications for snowline reconstruction. *Quaternary Research* 42:359–62.

Clark, D. H., E. J. Steig, N. Potter, and A. R. Gillspie. 1998. Genetic variability of rock glaciers. *Geografiska Annaler* 80A:175–82.

Dawson, R. J., A. T. Werner, and T. Q. Murdock. 2008. *Preliminary analysis of climate change in the Cariboo-Chilcotin area of British Columbia*. Victoria BC: Pacific Climate Impacts Consortium, University of Victoria. 49.

Delaloye, R., S. Morard, C. Barboux, D. Abbet, V. Gruber, M. Riedo, and S. Gachet. 2013. Rapidly moving rock glaciers in Mattertal. In *Mattertal–Ein Tal in Bewegung*, C. Graf. ed., 21–31. Birmensdorf: Eidg. Forschungsanstalt WSL.

Delaloye, R., E. Perruchoud, M. Avian, V. Kaufmann, H. Bodin, A. Ikeda, A. Kääb, A. Kellerer-Piklbauer, K. Krainer, C. Lambiel, et al., 2008: Recent interannual variations of rock glacier creep in the European Alps. In *Ninth International Conference on Permafrost*, Fairbanks, AK, 343–48.

Esper Angillieri, M. Y. E. 2010. Application of frequency ratio and logistic regression to active rock glacier occurrence in the Andes of San Juan, Argentina. *Geomorphology* 114:396–405.

Etzelmuller, B., and J. O. Hagen. 2005. Glacier-permafrost interaction in arctic and alpine mountain environments with examples from southern Norway and Svalbard. In *Cryospheric Systems: Glaciers and Permafrost*, eds. C. Harris, and J. B. Murton., Vol. 242, 11–27. London: Geological Society, Special Publications.

Falconer, G., W. E. S. Henoch, and G. M. Østrem. 1965. A glacier map of southern British Columbia and Alberta. *Geographical Bulletin* 8:108–12.

Francou, B., and L. Reynaud. 1992. Ten years of surficial velocities on a rock glacier (Laurichard, French Alps). *Permafrost and Periglacial Processes* 3:209–13.

Frehner, M., A. H. M. Ling, and I. Gärtner-Roer, 2014: Furrow and ridge morphology on rockglaciers explained by gravity driven buckle folding: A case study from the Murtèl Rockglacier (Switzerland). *Permafrost and Periglacial Processes*. Published online in Wiley Online Library.

French, H. M., and O. Slaymaker. 1993. *Canada's Cold Environments*, Vol. 1. Montreal, QC: McGill Queen's University Press.

Gardner, J. 1978. Wenkchemna Glacier: Ablation complex and rock glacier in the Canadian Rocky Mountains. *Canadian Journal of Earth Sciences* 15:1200–04.

Geogratis. 2013. Canadian Digital Elevation Model Product Specifications, Edition 1.1. Government of Canada, Natural Resources Canada, Map Information Branch, Sherbrooke, Quebec. http://ftp.geogratis.gc.ca/pub/nrcan_rncan/elevation/cdem_mnec/ doc/CDEM_product_specs.pdf.

Giardino, J. R., J. F. Shroder, and M. P. Lawson. 1984. Tree-ring analysis of movement of a rock glacier complex on Mount Mestas, Colorado, U.S.A. *Arctic, Antarctic, and Alpine Research* 16:299–309.

Gorbunov, A. P., 1983: Rock glaciers of the mountains of Middle Asia. In *Proceedings of the Fourth International Conference on Permafrost*. National Academy Press: Washington, 359–62.

Gorbunov, A. P., S. N. Titkov, and V. G. Polyakov. 1992. Dynamics of rock glaciers of the northern Tien Shan and the Djungar Ala Tau, Kazakhstan. *Permafrost and Periglacial Processes* 3:29–39.

Grissino-Mayer, H. D. 2001. Evaluating crossdating accuracy: A manual and tutorial for the computer program COFECHA. *Tree-Ring Research* 57:205–21.

Grubb, M. C., 2006: *Evidence for a late Pleistocene alpine glacier advance in the middle Coast Mountains, British Columbia*. B.Sc. thesis, Geography Program, University of Northern British Columbia, Prince George, British Columbia.

Guay, R., R. Gagnon, and H. Morin. 1992. A new automatic and interactive tree-ring measurement system based on a line scan camera. *The Forestry Chronicle* 38:138–41.

Haeberli, W. 1985. Creep of mountain permafrost: Internal structure and flow of Alpine rock glaciers. *Mitteilungen Der Versuchsanstalt Fur Wasserbau, Hydrologie Und Glaziologie an Der ETH Zurich* 77:5–142.

Haeberli, W., B. Hallet, L. Arenson, R. Elconin, O. Humlum, A. Kääb, V. Kaufmann, B. Ladanyi, N. Matsuoka, S. Springman, et al. 2006. Permafrost creep and rock glacier dynamics. *Permafrost and Periglacial Processes* 17:189–214.

Harris, S. A. 1981. Climatic relationships of permafrost zones in areas of low winter snow-cover. *Arctic* 34:64–70.

Harris, S. A., and R. J. E. Brown, 1981: Permafrost distribution along the Rocky Mountains in Alberta. *Proceedings from the Fourth Canadian Permafrost Conference*, pp. 59–67.

Hasler, M., M. Geertsma, and M. Hoelzle, 2014: *Permafrost favourability map of British Columbia*. Conference Abstract, Geological Society of America Annual Meeting, Vancouver, British Columbia.

Hausmann, H., K. Krainer, E. Brückl, and W. Mostler. 2007. Internal structure and ice content of Reichenkar rock glacier (Stubai Alps, Austria) assessed by geophysical investigations. *Permafrost and Periglacial Processes* 18:351–67.

Heginbottom, J. A. 2002. Permafrost mapping: A review. *Progress in Physical Geography* 26:623–42.

Heginbottom, J. A., M. A. Dubreuil, and P. A. Harker. 1995. Canada Permafrost, Sheet MCR 4177. *The National Atlas of Canada*, 5th. Ottawa: Natural Resources Canada.

Hoadley, R. B. 1990. *Identifying Wood: Accurate Results with Simple Tools*. Newton, CT: The Taunton Press.

Holmes, R. L. 1983. Computer-assisted quality control in tree-ring dating and measurement. *Tree-Ring Bulletin* 43:69–78.

Humlum, O. 1982. Rock glacier types on Disko, central West Greenland. *Geografisk Tidsskrift* 82:59–66.

Humlum, O. 1984. Altitudinal trends of talus-derived lobate rock glaciers on Disko, central West Greenland. *Geografisk Tidsskrift* 84:35–39.

Humlum, O. 1996. Origin of rock glaciers: Observations from Mellemfjord, Disko Island, central West Greenland. *Permafrost and Periglacial Processes* 7:361–80.

Humlum, O. 1997. Active layer thermal regime and three rock glaciers in Greeland. *Permafrost and Periglacial Processes* 8:383–408.

Humlum, O. 1998. The climatic significance of rock glaciers. *Permafrost and Periglacial Processes* 9:375–95.

Humlum, O. 2000. The geomorphic significance of rock glaciers: Estimates of rock glacier debris volumes and headwall recession rates in West Greenland. *Geomorphology* 35:41–67.

Ikeda, A., N. Matsuoka, and A. Kääb. 2008. Fast deformation of perennially frozen debris in a warm rock glacier in the Swiss Alps: An effect of liquid water. *Journal of Geophysical Research* 113:1–12.

Janke, J. R. 2005. Long-term flow measurements (1961-2002) of the Arapaho, Taylor, and Fair rock glaciers, Front Range, Colorado. *Physical Geography* 26:313–36.

Janke, J. R., N. R. Regmi, J. R. Giardino, and J. D. Vitek. 2013. 8.17 Rock Glaciers. In *Treatise on Geomorphology, Volume 8: Glacial and Periglacial Geomorphology*, J. R. Giardino, and J. M. Harbor. eds., 238–73. San Diego: Elsevier Academic Press.

Johnson, B. G., G. D. Thackray, and R. van Kirk. 2007. The effect of topography, latitude, and lithology on rock glacier distribution in the Lemhi Range, central Idaho, USA. *Geomorphology* 91:38–50.

Johnson, P. G. 1978. Rock glacier types and their drainage systems, Grizzly Creek, Yukon Territory. *Canadian Journal of Earth Sciences* 15:1496–507.

Johnson, P. 1980. Glacier-rock glacier transition in the Southwest Yukon Territory, Canada. *Arctic and Alpine Research* 12:195–204.

Journeay, J. M., and R. M. Friedman. 1993. The Coast Belt thrust system: Evidence of Late Cretaceous shortening in southwest British Columbia. *Tectonics* 12:756–75.

Kääb, A. 1996. Photogrammetrische Analyse zur Früherkennung gletscher- und permafrostbedingter Naturgefahren im Hochgebirge. *Mitteilungen Der VAW/ ETH Zürich* 145:181.

Kääb, A. 1997. Oberflächenkinematik ausgewählter Blockgletscher des Oberengadins. Beiträge aus der Gebirgs-Geomorphologie. *Mitteilung Der VAW-ETH Zürich* 158:121–40.

Kääb, A., and C. Kneisel. 2006. Permafrost creep within a recently deglaciated glacier forefield: Muragl, Swiss Alps. *Permafrost and Periglacial Processes* 17:79–85.

Kääb, A., and M. Weber. 2004. Development of transverse ridges on rock glaciers: Field measurements and laboratory experiments. *Permafrost and Periglacial Processes* 15:379–91.

Kirkbride, M. 2011. Debris-covered glaciers. In *Encyclopedia of Snow, Ice, and Glaciers*, V. P. Singh, P. Singh, and U. K. Haritashya. eds., 190–92. Netherlands: Springer.

Kneisel, C., and A. Kääb. 2007. Mountain permafrost dynamics within a recently exposed glacier forefield inferred by a combined geomorphological, geophysical and photogrammetrical approach. *Earth Surface Processes and Landforms* 32:1797–810.

Koning, D. M., and D. J. Smith. 1999. Movement of Kings Throne rock glacier, Mount Rae area, Canadian Rocky Mountains. *Permafrost and Periglacial Processes* 10:151–62.

Krainer, K., and W. Mostler. 2000. Reichenkar rock glacier: A glacier derived debris-ice system in the western Stubai Alps, Austria. *Permafrost and Periglacial Processes* 11:267–75.

Krummenacher, B., K. Budmiger, D. Mihajlovic, and B. Blank. 1998. Periglaziale Prozesse und Formen im Furggentälti, Gemmipass. In *Analysen zur räumlich-zeitlichen Entwicklung der Permafrostverbreitung und der Solifluktion, basierend auf der Entwicklung und Anwendung moderner Arbeitsmethoden*, 245. Davos Dorf: Mitteilungen des

Eidgenössisches Institutes für Schnee-und Lawinenforschung.

Larocque, S. J., and D. J. Smith. 2003. Little Ice Age glacial activity in the Mt. Waddington area, British Columbia Coast Mountains, Canada. *Canadian Journal of Earth Sciences* 40:1413–36.

Larocque, S. J., and D. J. Smith. 2005a. A dendroclimatological reconstruction of climate since AD 1700 in the Mt. Waddington area, British Columbia Coast Mountains, Canada. *Dendrochronologia* 22:93–106.

Larocque, S. J., and D. J. Smith. 2005b. 'Little Ice Age' proxy glacier mass balance records reconstructed from tree rings in the Mt Waddington area, British Columbia Coast Mountains, Canada. *The Holocene* 15:748–57.

Lilleøren, K. S., and B. Etzelmuller. 2011. A regional inventory of rock glaciers and ice-cored moraines in Norway. *Geografiska Annaler* 93A:175–91.

Lilleøren, K. S., B. Etzelmüller, I. Gärtner-Roer, A. Kääb, S. Westermann, and Á. Guðmundsson. 2013a. The distribution, thermal characteristics and dynamics of permafrost in Tröllaskagi, Northern Iceland, as inferred from the distribution of rock glaciers and ice-cored moraines. *Permafrost and Periglacial Processes* 24:322–35.

Lilleøren, K. S., O. Humlum, A. Nesje, and B. Etzelmüller. 2013b. Holocene development and geomorphic processes at Omnsbreen, southern Norway: Evidence for glacier–Permafrost interactions. *The Holocene* 23:796–809.

Luckman, B. H., and K. J. Crockett. 1978. Distribution and characteristics of rock glaciers in the southern part of Jasper National Park, Alberta. *Canadian Journal of Earth Sciences* 15: 540–50.

Margold, M., K. N. Jansson, J. Kleman, A. P. Stroeven, and J. J. Clague. 2013. Retreat pattern of the Cordilleran Ice Sheet in central British Columbia at the end of the last glaciation reconstructed from glacial meltwater landforms. *Boreas* 42:830–47.

Martin, H. E., and W. B. Whalley. 1987. Rock glaciers part 1: Rock glacier morphology: Classification and distribution. *Progress in Physical Geography* 11:260–82.

Massey, N. W. D., J. W. MacIntyre, P. J. Desjardins, and R. T. Cooney, 2005: *Ministry of Energy and Mines, Geofiles*. Available at: http://www.empr.gov.bc.ca/Mining/Geoscience/BedrockMapping/Pages/BCGeoMap.aspx

Menounos, B., G. Osborn, J. J. Clague, and B. H. Luckman. 2009. Latest Pleistocene and Holocene glacier fluctuations in western Canada. *Quaternary Science Reviews* 28:2049–74.

Monger, J. W. H., and J. M. Journeay. 1994. Guide to the geology and tectonic evolution of the southern Coast Mountains. In *Geological Survey of Canada Open File 2490*, 77. Ottawa, Ontario: Geological Survey of Canada.

Monnier, S., C. Camerlynck, F. Rejiba, C. Kinnard, and P. Y. Galibert. 2013. Evidencing a large body of ice in a rock glacier, Vanoise Massif, Northern French Alps. *Geografiska Annaler* 95A:109–23.

Monnier, S., and C. Kinnard. 2015. Reconsidering the glacier to rock glacier transformation problem: New insights from the central Andes of Chile. *Geomorphology* 238:47–55.

Mood, B. J., and D. J. Smith. 2015. Holocene glacier activity in the British Columbia Coast Mountains, Canada. *Quaternary Science Reviews* 128:14–36.

Mustard, P. S., and P. van der Heyden. 1997. Geology of Tatla Lake (92N/15) and the east half of Bussel Creek (92N/14) map areas. *Geological Survey of Canada, Paper* 2:103–18.

Ødegard, R. S., K. Isaksen, T. Eiken, and J. L. Sollid. 2003. Terrain analyses and surface velocity measurements of the Hiorthfjellet rock glacier, Svalbard. *Permafrost and Periglacial Processes* 14:359–65.

Osborn, G. 1975. Advancing rock glacier in the Lake Louise area, Banff National Park. *Canadian Journal of Earth Sciences* 12:1060–62.

Østrem, G. 1966. The height of the glaciation limit in southern British Columbia and Alberta. *Geografiska Annaler* 48A:126–38.

Østrem, G., and K. Arnold. 1970. Ice-cored moraines in southern British Columbia and Alberta, Canada. *Geografiska Annaler* 52A:120–28.

Pillewizer, W. 1957. Untersuchungen an Blockströmen der Ötztaler Alpen. *Abhandlungen Des Geographischen Institutes Der Freie UniversitäT Berlin* 5:37–50.

Potter, N., Jr. 1972. Ice-cored rock glacier, Galena Creek, Northern Aksaroka Mountains, Wyoming. *Geological Society of America Bulletin* 83:3025–58.

Racoviteanu, A. E., F. Paul, B. Raup, S. J. S. Khalsa, and R. Armstrong. 2009. Challenges and recommendations in mapping of glacier parameters from space: Results of the 2008 Global Land Ice Measurements from Space (GLIMS) workshop, Boulder, Colorado, USA. *Annals of Glaciology* 50(53):53–69.

Rangecroft, S., S. Harrison, K. Anderson, J. Magrath, A. P. Castel, and P. Pacheco. 2014. A First rock glacier inventory for the Bolivian Andes. *Permafrost and Periglacial Processes* 25:333–43.

Ribolini, A., and D. Fabre. 2006. Permafrost existence in the rock glaciers of the Argentera Massif (Maritime Alps, Italy). *Permafrost and Periglacial Processes* 17:49–63.

Roddick, J. A. 1983. Geophysical review and composition of the Coast Plutonic Complex, south of latitude 55°N. *Circum-Pacific Plutonic Terranes: Geological Society of America Memoir* 159:195–211.

Rodenhuis, D. R., K. E. Bennett, A. T. Werner, T. Q. Murdock, and D. Bronaugh. 2007. Hydro-climatology and future climate impacts in British Columbia. In *Pacific Climate Impacts Consortium*, 1–132. Victoria: University of Victoria.

Roer, I. 2005. *Rockglacier kinematics in a high mountain geosystem*. PhD diss., Universitäts-und Landesbibliothek Bonn.

Roer, I., W. Haeberli, M. Avian, V. Kaufmann, R. Delaloye, C. Lambiel, and A. Kääb. 2008. Observations and considerations on destabilizing active rock glaciers in the European Alps. *Ninth International Conference on Permafrost*, 1505–10.

Rusli, N., M. R. Majid, and A. H. M. Din. 2014. Google Earth's derived digital elevation model: A comparative assessment with Aster and SRTM data. *IOP Conference Series: Earth and Environmental Science* 18:1–6.

Schiefer, E., B. Menounos, and R. Wheate. 2007. An inventory and morphometric analysis of British Columbia glaciers, Canada. *Journal of Glaciology* 54:551–60.

Schmid, M.-O., P. Baral, S. Gruber, S. Shahi, T. Shrestha, D. Stumm, and P. Wester. 2014. Assessment of permafrost distribution maps in the Hindu Kush-Himilayan region

using rock glaciers mapped in Google Earth. *The Cryosphere Discussions* 8:5293–319.

Schneider, B., and H. Schneider. 2001. Zur 60jährigen Messreihe der kurzfristigen Geschwindigkeitsschwankungen am Blockgletscher im Äusseren Hochebenkar, Ötztaler Alpen, Tirol. *Zeitschrift FüR Gletscherkunde Und Glazialgeologie* 37:1–33.

Scotti, R., F. Brardinoni, S. Alberti, P. Frattini, and G. B. Crosta. 2013. A regional inventory of rock glaciers and protalus ramparts in the central Italian Alps. *Geomorphology* 186:136–49.

Seppi, R., T. Zanoner, A. Carton, A. Bondesan, R. Francese, L. Cartura, M. Zumiani, M. Giorgi, and A. Ninfo. 2015. Current transition from glacial to periglacial processes in the Dolomites (South-Eastern Alps). *Geomorphology* 228:71–86.

Sherzer, W. H. 1907. Glaciers of the Canadian Rockies and Selkirks (Smithsonian Expedition of 1904). *Smithsonian Institution, No. 1692*. Washington, DC.

Shroder, J. F. 1978. Dendrogeomorphological analysis of mass movement on Table Cliffs Plateau, Utah. *Quaternary Research* 9:168–85.

Sloan, V. F., and L. D. Dyke. 1998. Decadal and millennial velocities of rock glaciers, Selwyn Mountains, Canada. *Geografiska Annaler* 80A:237–49.

Sorg, A., A. Kääb, A. Roesch, C. Bigler, and M. Stoffel. 2015. Contrasting responses of Central Asian rock glaciers to global warming. *Nature Research Journal: Scientific Reports* 5:8228.

Spittlehouse, D., and T. Wang. 2014. *Evaluation of ClimateBC V5*. Retrieved from http://climatemodels.forestry.ubc.ca/climatebc/downloads/ClimateBCv5_evaluation.pdf

Starheim, C. C. A., D. J. Smith, and T. D. Prowse. 2013. Multi-century reconstructions of Pacific salmon abundance from climate-sensitive tree rings in west central British Columbia, Canada. *Ecohydrology* 6:228–40.

Steinman, B. A., M. B. Abbott, M. E. Mann, J. D. Ortiz, S. Feng, D. P. Pompeani, N. D. Stansell, L. Anderson, B. P. Finney, and B. W. Bird. 2014. Ocean-atmosphere forcing of centennial hydroclimate variability in the Pacific Northwest. *Geophysical Research Letters* 41:2553–60.

Umhoefer, P. J., and P. Schiarizza. 1996. Latest Cretaceous to early Tertiary dextral strike-slip faulting on the southeastern Yalakom fault system, southeastern Coast Belt, British Columbia. *Geological Society of America Bulletin* 108:768–85.

van der Heyden, P., P. S. Mustard, and R. Friedman. 1994. Northern continuation of the Eastern Waddington Thrust Belt and Tyaughton Trough, Tatla Lake-Bussel Creek map areas, west-central British Columbia. In *Current Research 1994-A, Cordillera and Pacific Margin*, 87–94. Ottawa, Ontario: Geological Survey of Canada.

VanLooy, J. A., and R. R. Forster. 2008. Glacial changes of five southwest British Columbia icefields, Canada, mid-1980s to 1999. *Journal of Glaciology* 54(186):469–78.

Wahrhaftig, C., and A. Cox. 1959. Rock glaciers in the Alaska Range. *Geological Society of America Bulletin* 70:383–436.

Wang, T., A. Hamann, D. L. Spittlehouse, and S. N. Aitken. 2006. Development of scale-free climate data for Western Canada for use in resource management. *International Journal of Climatology* 26:383–97.

Wang, T., A. Hamann, D. L. Spittlehouse, and T. Q. Murdock. 2012. ClimateWNA-High-resolution spatial climate data for western North America. *Journal of Applied Meteorology and Climatology* 51:16–29.

White, S. E. 1971. Rock glacier studies in the Colorado Front Range, 1961 to 1968. *Arctic and Alpine Research* 3(1):43–64.

White, S. E. 1987. Differential movement across transverse ridges on Arapaho rock glacier, Colorado, Front Range, USA. In *Rock Glaciers*, J. R. Giardino, J. F. Shroder Jr, and J. D. Vitek. eds., 145–49. London: Allen and Unwin.

Wood, L. J., D. J. Smith, and M. N. Demuth. 2011. Extending the Place Glacier mass-balance record to AD 1585, using tree rings and wood density. *Quaternary Research* 76:305–13.